Climatic Effects of Air Pollutants over China: A Review

LIAO Hong*, CHANG Wenyuan, and YANG Yang

State Key Laboratory of Atmospheric Boundary Layer Physics and Atmospheric Chemistry (LAPC),

Institute of Atmospheric Physics, Chinese Academy of Sciences, Beijing 100029

ABSTRACT

Tropospheric ozone (O_3) and aerosols are major air pollutants in the atmosphere. They have also made significant contributions to radiative forcing of climate since preindustrial times. With its rapid economic development, concentrations of air pollutants are relatively high in China; hence, quantifying the role of air pollutants in China in regional climate change is especially important. This review summarizes existing knowledge with regard to impacts of air pollutants on climate change in China and defines critical gaps needed to reduce the associated uncertainties. Measured monthly, seasonal, and annual mean surface-layer concentrations of O_3 and aerosols over China are compiled in this work, with the aim to show the magnitude of concentrations of O_3 and aerosols over China and to provide datasets for evaluation of model results in future studies. Ground-based and satellite measurements of O_3 column burden and aerosol optical properties, as well as model estimates of radiative forcing by tropospheric O_3 and aerosols are summarized. We also review regional and global modeling studies that have investigated climate change driven by tropospheric O_3 and/or aerosols in China; the predicted sign and magnitude of the responses in temperature and precipitation to O_3/aerosol forcings are presented. Based on this review, key priorities for future research on the climatic effects of air pollutants in China are highlighted.

Key words: tropospheric ozone, aerosols, radiative forcing, climate change

Citation: Liao, H., W. Y. Chang, and Y. Yang, 2015: Climatic effects of air pollutants over China: A review. *Adv. Atmos. Sci.*, **32**(1), 115–139, doi: 10.1007/s00376-014-0013-x.
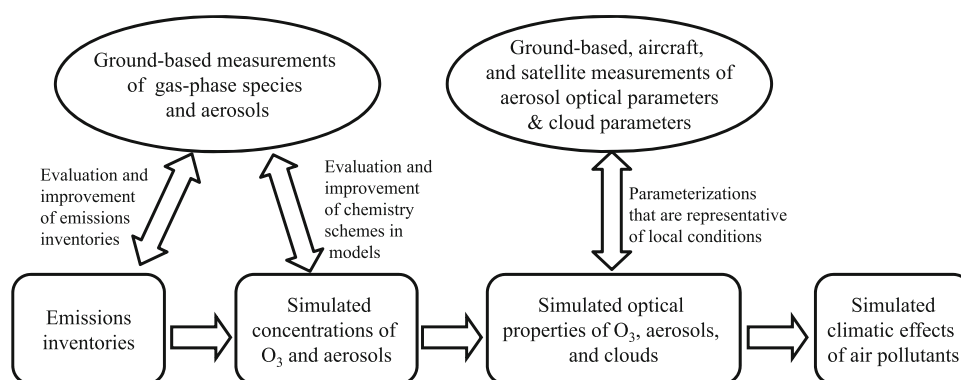
1. Introduction

Tropospheric O_3 and aerosols are major air pollutants in the atmosphere that have adverse effects on human health, crops, plants, and atmospheric visibility. They have also made significant contributions to radiative forcing of climate since preindustrial times. Ozone is a greenhouse gas, with a global mean anthropogenic radiative forcing of 0.40 (0.20 to 0.60) W m^{-2} (IPCC, 2013). Aerosols influence climate through aerosol-radiation interactions (direct effect) and aerosol-cloud interactions (indirect effect). Anthropogenic changes in aerosols are estimated to have a global mean total direct radiative forcing of -0.45 (-0.95 to $+0.05$) W m^{-2} and an indirect radiative forcing of -0.45 (-1.2 to 0.0) W m^{-2}, which are comparable in magnitude to the global mean radiative forcing of 2.83 (2.26 to 3.40) W m^{-2} by the increases in CO_2, CH_4, N_2O and halocarbons from preindustrial times (IPCC, 2013). With its rapid economic development, concentrations of air pollutants are relatively high in China, suggesting that the climatic effects of air pollutants in China could be much more significant than those represented by the global mean radiative forcing values in IPCC (2013).

Climatic effects of air pollutants in China have unique features, because China is located within a large monsoon domain. In May to September every year, Asian summer monsoon prevails; strong cross-equatorial winds flow from the Southern Hemisphere (SH) to the Northern Hemisphere (NH), bringing warm and moist air from the oceans to eastern China. Rain belts and the associated deep convection that stretch for thousands of kilometers move from southeastern to northern China during this period. In the months from November to March, Asian winter monsoon prevails; strong northerlies in high latitudes bring cold and dry air to eastern China. While the seasonal and interannual variations in meteorological fields associated with Asian monsoon can influence air pollutants over eastern China by influencing their transport, chemical reactions, and deposition (Zhang et al., 2010; Yan et al., 2011; Zhu et al., 2012), aerosols have been shown to have large impacts on Asian summer monsoon (Menon et al., 2002; Ramanathan et al., 2005; Lau and Kim, 2006; Bollasina et al., 2011). These complex feedbacks among chemistry and regional climate have to be considered in studies that examine the climatic effects of air pollutants.

Estimates of the climatic effects of air pollutants have to rely on climate models. The commonly used approach to quantify the climatic effects of air pollutants is shown in Fig. 1. Concentrations of air pollutants are simulated in coupled chemistry–aerosol–climate models using emissions invento-

---

* Corresponding author: LIAO Hong

Email: hongliao@mail.iap.ac.cn

Fig. 1. Approach for estimating the climatic effects of air pollutants.

ries, and then optical properties of tropospheric O_3, aerosols, and clouds are calculated depending on the chemical and physical properties of air pollutants. After the evaluation of simulated concentrations and optical properties by comparisons with measurements, climatic effects of air pollutants are obtained by examining the differences in simulated climate with or without the optical properties of pollutants in the radiative transfer scheme of climate models. During the past decade, important advances have been made in understanding air pollutants and their roles in climate change in China. Emissions inventories of NO_x, CO, speciated volatile organic compounds (VOCs), SO_2, NH_3, black carbon (BC), and organic carbon (OC) have become available for the Chinese domain (Streets et al., 2003), allowing concentrations of O_3 and different aerosol species to be simulated and their climatic effects estimated by using numerical models. Increasing ground-based and aircraft measurements of concentrations of O_3 and speciated aerosols in China, together with satellite measurements of the physical and optical properties of aerosol particles, have provided datasets to evaluate model predictions and to improve simulations for the quantitative assessment of climatic effects of O_3 and aerosols (Li et al., 2007c; Li et al., 2011b).

This review summarizes recent advances in our understanding of the climatic effects of air pollutants in China. All the key datasets or parameters needed for quantifying the effects of air pollutants on climate are reviewed. The available emissions inventories for the simulation of O_3 and aerosols are introduced in section 2. The measured surface-layer concentrations of O_3 and aerosols and column burdens of O_3 in China are summarized in section 3. The observed optical properties of aerosols, including aerosol optical depth (AOD) and single scattering albedo (SSA), are presented in section 4. Section 5 describes the correlations between air pollutants and observed changes in meteorological parameters in China. Estimates of radiative forcing by O_3 and different aerosol species are presented in section 6. Modeling studies on the impacts of air pollutants on climate change in China are reviewed in section 7. Finally, the key priorities for future research on the climatic effects of air pollutants in China are highlighted in section 8.

2. Emissions inventories for the simulation of tropospheric O_3 and aerosols

Emissions inventories allow us to quantify the anthropogenic contribution to climate change, understand the role of each chemical species in the climate system, and eventually take measures to mitigate climate change. Emissions of CH_4, NO_x, CO, and non-methane volatile organic compounds (NMVOCs) are needed for the simulation of tropospheric O_3, and those of SO_2, NH_3, BC, and OC are essential for the simulation of aerosols. Emissions of chemical species come from both anthropogenic and natural sources. Natural emissions include lightning NO_x, NO_x from soil, biogenic hydrocarbons, BC and OC from wild fires, dimethyl sulphide, sea spray, and mineral dust.

Figure 2 shows the changes in emissions of NO_x, SO_2, NH_3, BC and OC during the years 1850–2010 from human activities (power, industry, transportation, residential and agricultural activities) and biomass burning, which are taken from the IPCC Fifth Assessment Report (AR5) emissions inventories. The global total emission of SO_2 peaked in 1980 when emissions in Europe and North America were the highest, and the global total emissions of NO_x and NH_3 peaked in 1990. Emissions of all species in eastern China have been increasing largely since 1950. In 2000, the emissions of NO_x, SO_2, NH_3, BC and OC in eastern China accounted for, respectively, 11.2%, 18.8%, 11.6%, 17.3%, and 8.7% of global total emissions.

The NMVOCs are important precursors of tropospheric O_3 and secondary organic aerosol, although they are not shown in Fig. 2. Bo et al. (2008) reported that anthropogenic NMVOCs emissions in China increased from 3.91 Tg in 1980 to 16.49 Tg in 2005 because of the rapid growth in the number of automobiles and solvent and paint use in China. Emissions from natural vegetation are also large sources of VOCs. The estimated annual emission of biogenic VOCs (including isoprene, monoterpenes, and other reactive VOCs) in China averaged over the period 2001–06 was 18.85 TgC yr^{-1} (Fu and Liao, 2012), which was comparable in magnitude to anthropogenic emissions.

It should be noted that emissions inventories contain large

uncertainties. For example, Streets and Aunan (2005) found BC emissions in China peaked in 1994–95 and showed reductions in 1996–2000 as a result of the reduced usage of biofuels and coal in residential and industrial sectors. However, Lei et al. (2011) reported that there were no significant trends in emissions of BC and OC in China during 1990–2000; emissions of BC and OC increased after 2000, with peak values of 1.51 Tg and 3.19 Tg, respectively, in 2005. Few previous studies have quantified the impacts of uncertainties in emissions on simulated climate.
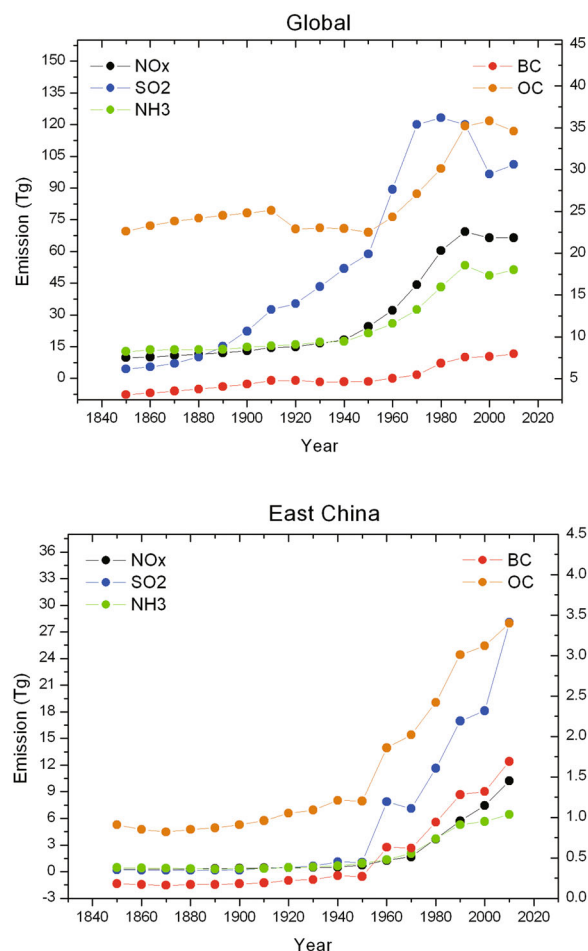
3. Observed levels of ozone and aerosols over China

Measurements of O_3 and speciated aerosols are important for understanding the uncertainties in emissions inventories and simulated concentrations, which can also help to improve the representation of chemical processes in models (Fig. 1). To examine the climatic effects of air pollutants, long-term measurements of concentrations are needed; monthly, seasonal, or annual mean concentrations are usually used in evaluations of model simulations. Such measurements at ground stations are very limited in China, since most previous field campaigns were designed for air quality studies, focusing on the high concentrations of air pollutants in urban and suburban regions for certain short periods of time. For aerosols, the long-term measurements that are available, managed by the Ministry of Environmental Protection of the People's Republic of China (http://datacenter.mep.gov.cn/TestRunQian/air_dairy.jsp), are PM_{10} mass concentrations, which can hardly be used for studies of the climatic effect of aerosols because the optical properties of aerosols are mainly determined by $PM_{2.5}$ instead of PM_{10} particles. Based on the available literature, we summarize in this section the measured monthly to annual mean levels of tropospheric O_3 and aerosols.

3.1. Tropospheric ozone

3.1.1. Ground-based measurements

Table 1 summarizes ground-based measurements of O_3 in China. Observed seasonal or annual mean O_3 concentrations in China were mostly in the range of 20–60 ppbv. The background O_3 concentrations are relatively higher in western China as a result of the transport of O_3 from the stratosphere (Wang et al., 2006a). For example, concentrations at Waliguan (36.3°N, 100.9°E) were in the range of 40–60 ppbv, which were higher than the measured values at other background stations such as Fenghuanshan (40.5°N, 124°E), Lin'an (31.3°N, 120.4°E), and Long Feng Mountain (44.7°N, 127.6°E). Concentrations of O_3 in eastern China are influenced largely by anthropogenic emissions (Wang et al., 2011). Based on 810 vertical profiles of O_3 measured by aircraft in different seasons during 1995–2005, Ding et al. (2008) showed that the average mixing ratio of O_3 in Beijing increased from about 40 ppbv at the ground to about 50 ppbv at 2 km altitude. Ding et al. (2008) also compared the

Fig. 2. Annual emissions [teragram (Tg) = 1.0×10^{12} gram] of NO_x, SO_2, NH_3, BC, and OC from human activities (power, industry, transportation, residential and agricultural activities) and biomass burning taken from the IPCC AR5 emissions inventories. The top panel shows global total emissions and the bottom panel shows total emissions summed over eastern China (29°–35°N, 102.5°–122.5°E). The y-axis on the left is for emissions of NO_x, SO_2 and NH_3, while that on the right is for emissions of BC and OC. Emissions in 2010 are taken from the IPCC AR5 RCP4.5 scenario. Biomass burning emissions during 1850–90 are the same as the values in 1900.

observed O_3 concentrations in Beijing with measurements in Tokyo, Paris, and New York, and reported that O_3 concentrations in the lower troposphere in Beijing were generally 5–10 ppbv higher than those in Tokyo and New York. In July to September of 2001–06, the average measured O_3 concentrations at six urban sites in Beijing was 26.6 ± 2.8 ppbv (Tang et al., 2009). With respect to the long-term trend of O_3, surface concentrations measured in Linan, a background station in eastern China, showed that the monthly highest 5% ozone concentrations increased over the period 1991–2006 (Xu et al., 2008).

3.1.2. Column burdens

Estimates of the climatic effect of O_3 rely upon not only surface concentrations but also vertical distributions and col-

Table 1. Ground-based measurements of ozone in China.

Location	Period		Mixing ratio (ppbv)	Reference
Beijing (39.9°N, 116.5°E)	1995–2005		40	Ding et al. (2008)
	July to September of 2001–06		26.6 ± 2.8	Tang et al (2009)
	20 June to 16 September 2007		36.2–58.2	Xu et al. (2011)
Miyun (40.5°N, 116.8°E)	2005–07	Spring	50–55	Wang et al. (2011)
		Summer	85 (June)	Wang et al. (2011)
		Autumn	65 (September)	Wang et al. (2011)
		Winter	50–55	Wang et al. (2011)
Shangdianzi (40.7°N, 117.1°E)	2004–06	Spring	35.0–41.4	Lin et al. (2008)
		Summer	30.9–46.5	Lin et al. (2008)
		Autumn	19.4–34.7	Lin et al. (2008)
		Winter	17.7–27.0	Lin et al. (2008)
	September to December 2003		26.8 ± 13.9	Meng et al. (2009)
	January to December 2004		30.1 ± 21.0	Meng et al. (2009)
	January to December 2005		32.8 ± 19.1	Meng et al. (2009)
	January to December 2006		30.9 ± 19.8	Meng et al. (2009)
Nanjing (32.0°N, 118.5°E)	2000–2003	Spring	27.0	Tu et al. (2007)
		Summer	22.8	Tu et al. (2007)
		Autumn	18.4	Tu et al. (2007)
		Winter	14.1	Tu et al. (2007)
Qingdao (36.5°N, 121°E)	24 February to 15 March 2002		26.6	Takami et al. (2006)
	16–28 February 2001		23.5	Takami et al. (2006)
	15–28 January 2000		35.9	Takami et al. (2006)
Qingdao (36.1°N, 120.5°E)	December 1994		23	Li et al. (1999)
	June 1995		35	Li et al. (1999)
Fenghuanshan (40.5°N, 124°E)	16 February to 2 March 2001		30.2	Takami et al. (2006)
	13–25 January 2000		32.2	Takami et al. (2006)
Waliguan, Tibetan Plateau (36.3°N, 100.9°E)	20 April to 23 May and 15	Spring	58 ± 9	Wang et al. (2006a)
	July to 16 August 2003	Summer	54 ± 11	Wang et al. (2006a)
	August 1994 to July 1995	Spring	52.2 ± 4.21	Yan et al. (1997)
		Summer	60.9 ± 6.87	Yan et al. (1997)
		Autumn	42.1 ± 4.16	Yan et al. (1997)
		Winter	42.4 ± 2.73	Yan et al. (1997)
Lin'an (31.3°N, 120.4°E)	December 1999		32	Yan et al. (2003)
	June 2000		40	Yan et al. (2003)
	August 1994 to July 1995	Spring	37.3 ± 5.89	Yan et al. (1997)
		Summer	32.9 ± 7.14	Yan et al. (1997)
		Autumn	39.84 ± 6.76	Yan et al. (1997)
		Winter	36.9 ± 9.08	Yan et al. (1997)
Chnshu (30.3°N, 119.4°E)	June 2000		45	Yan et al. (2003)
	December 1999		22	Yan et al. (2003)
Waliguan Mountain (36.3°N, 100.9°E)	September 1999 to June 2001		44.9	Carmichael et al. (2003)
Lin'an (30.3°N, 119.7°E)			38.3	Carmichael et al. (2003)
Shang Dian Zhi (40.7°N, 117.1°E)			38.0	Carmichael et al. (2003)
Cape D'Aequier (22.2°N, 114.3°E)			34.9	Carmichael et al. (2003)
Long Feng Mountain (44.7°N, 127.6°E)	August 1994 to July 1995	Spring	37.3 ± 5.89	Yan et al. (1997)
		Summer	32.9 ± 7.14	Yan et al. (1997)
		Autumn	39.84 ± 6.76	Yan et al. (1997)
		Winter	29.1 ± 3.00	Yan et al. (1997)
Gucheng (39.2°N, 115.7°E)	August 2009 to June 2010		19.4 ± 7.9	Wang et al. (2013)
Longtanhu (39.9°N, 116.4°E)	August 2009 to June 2010		19.8 ± 8.7	Wang et al. (2013)
Xinglong (40.4°N, 117.6°E)	August 2009 to June 2010		47.3 ± 11.5	Wang et al. (2013)

umn burdens. Ozonesonde datasets are available only at a number of sites in China (Chan et al., 2003; Ding et al., 2008). Satellite measurements [such as those from Global Ozone Monitoring Experiment (GOME), GOME-2, SCanning Imaging Absorption spectroMeter for Atmospheric CHartographY (SCIAMACHY), Ozone monitoring instrument (OMI), Tropospheric Emission Spectrometer (TES), and Infrared Atmospheric Sounding Interferometer (IASI)] have excellent spatial and temporal coverage, which are useful for analyses of the distributions and seasonal variations of tropospheric column O_3 concentration over China. Liu et al. (2006) presented the first directly retrieved global distribution of tropospheric column ozone from GOME ultraviolet measurements during December 1996 to November 1997. The retrieved column burdens clearly showed signals due to convection, biomass burning, stratospheric influence, pollution, and transport. Recently, using measurements from the IASI instrument aboard the European Metop-A satellite (launched in October 2006), Dufour et al. (2010) showed that maximum lower tropospheric O_3 (0–6 km partial column) occurs in late spring and early summer (May to June) in Beijing, and in early autumn in Shanghai and Hong Kong. Although biogenic emissions, temperature, and radiation are the highest in southeastern and southwestern China in July, O_3 concentra-

tions in those regions are generally low in summer because of the summer monsoon circulation that brings clean air from the oceans (Dufour et al., 2010).

3.2. Ground-based measurements of aerosols

Major aerosol species over China include sulfate (SO_4^{2-}), nitrate (NO_3^-), ammonium, elemental carbon (black carbon), primary organic carbon (POA), secondary organic carbon (SOA), and mineral dust aerosols. Measured $PM_{2.5}$ concentrations in China are compiled and listed in Table 2. In Beijing, ambient $PM_{2.5}$ concentrations ranged between 59.2 $\mu g\ m^{-3}$ (Wu and Wang, 2007) and 257.6 $\mu g\ m^{-3}$ (Dan et al., 2004). Simultaneous measurements of $PM_{2.5}$ concentrations in winter and summer of 2003 in 14 cities in China indicated that the average $PM_{2.5}$ concentration in these 14 cities was 163.9 $\mu g\ m^{-3}$ in winter and 71.2 $\mu g\ m^{-3}$ in summer (Cao et al., 2007). Over eastern China, aerosol concentrations are generally high in winter and low in summer, mainly caused by the large wet deposition of aerosols associated with the Asian summer monsoon (Zhang et al., 2010; Gao et al., 2011). Averaged over the 14 cities, carbonaceous aerosols (the sum of OC and BC) contributed to the $PM_{2.5}$ mass by 44.2% in winter and 38.8% in summer (Cao et al., 2007). Sulfate (Table 3) and nitrate (Table 4) aerosols also contribute

Table 2. Observed $PM_{2.5}$ concentrations in China.

Location	Concentrations ($\mu g\ m^{-3}$)		References
	Summer	Winter	
Beijing (39.9°N,116.5°E)	117.2 ± 48.3	126.5 ± 66.1	Cao et al. (2007)
	104.1 ± 45.1	175.9	He et al. (2001)
		257.6 ± 85.8	Dan et al. (2004)
	77.3 ± 55.7	135.7 ± 96.6	Sun et al. (2004)
	93.29 ± 56.26	214.23 ± 159.34	Wang et al. (2005b)
	88.99	122.09	Duan et al. (2006)
	107 ± 61	182 ± 107	Zhang et al. (2006)
	71	108	Xu et al. (2007)
	59.2		Wu and Wang (2007)
Changchun (45.5°N, 125.2°E)	59.6 ± 21.9	140.5 ± 28.6	Cao et al. (2007)
Chendu (30.7°N, 104°E)	114	225	Tao et al. (2013)
Jinsha (29.6°N, 114.2°E)	34.1	66.0	Zhang et al (2014)
Qingdao (36.0°N, 120.2°E)	30.1 ± 16.1	127.9 ± 58.5	Cao et al. (2007)
Tianjin (39.0°N, 117.1°E)	103.2 ± 27.9	179.4 ± 87.8	Cao et al. (2007)
Xi'an (34.2°N, 108.6°E)	130.8 ± 58.5	375.2 ± 143.5	Cao et al. (2007)
Yulin (38.2°N, 109.5°E)	50.5 ± 23.2	150.6 ± 77.3	Cao et al. (2007)
Chongqing (29.4°N, 106.3°E)	116.3 ± 38.1	311.8 ± 114.1	Cao et al. (2007)
Guangzhou (23.1°N, 113.1°E)	78.1 ± 29.7	105.9 ± 71.4	Cao et al. (2003, 2004)
	49.1 ± 9.3	156.0 ± 93.6	Cao et al. (2007)
		94.7	Tang et al. (2009)
Hong Kong (25.2°N, 115.1°E)	31 ± 16.9	54.5 ± 22.9	Cao et al. (2003, 2004)
	40.1 ± 14.0	64.0 ± 29.6	Cao et al. (2007)
Hangzhou (30.2°N, 120.1°E)	90.6 ± 40.8	168.6 ± 54.6	Cao et al. (2007)
Shanghai (31.1°N, 121.3°E)	52.2 ± 19.4	151.1 ± 95.4	Cao et al. (2007)
	35.85	93.91	Ye et al. (2003)
	59.7		Wu and Wang (2007)
	71.66 ± 28.20	76.09 ± 40.97	Wang et al. (2006b)
	50.02 ± 23.00	94.30 ± 44.10	Feng et al. (2009)
	15.10 ± 6.10	65.40 ± 16.80	Hou et al. (2011)
Nanjing (32.0°N, 118.5°E)	69.1	139.5	Huang et al. (2006)
Wuhan (30.4°N, 114.2°E)	70.8 ± 21.3	166.6 ± 72.7	Cao et al. (2007)
Xiamen (24.3°N, 118.0°E)	25.2 ± 15.8	70.2 ± 32.2	Cao et al. (2007)
Shenzhen (24.3°N, 114.1°E)	47.1 ± 16.7	60.8 ± 18.0	Cao et al. (2003, 2004)
Zhuhai (22.2°N, 113.3°E)	31.0 ± 20.0	59.3 ± 23.7	Cao et al. (2003, 2004)
Fuzhou (26.1°N, 119.3°E)	23.58	59.81	Xu et al. (2012)

Table 3. Observed concentrations of sulfate aerosol in China.

Location	Period		Concentration (µg m^{-3})	Reference
Beijing (39.9°N, 116.4°E)	24 November 1998 to 12 February 1999		30.8	Duan et al. (2004)
	July 1999 to September 2000	Summer	17.14	He et al. (2001)
		Autumn	12.55	He et al. (2001)
		Winter	24.87	He et al. (2001)
		Spring	10.15	He et al. (2001)
	2001–03	Spring	13.52	Wang et al. (2005b)
		Summer	18.42	Wang et al. (2005b)
		Autumn	12.69	Wang et al. (2005b)
		Winter	20.96	Wang et al. (2005b)
	August 2001 to September 2002	Average	9.90	Duan et al. (2006)
		Autumn	9.61	Duan et al. (2006)
		Winter	9.88	Duan et al. (2006)
		Spring	6.71	Duan et al. (2006)
		Summer	13.43	Duan et al. (2006)
	23 January to 14 February 2007		7.50	Ianniello et al. (2011)
	2–31 August 2007		18.24	Ianniello et al. (2011)
	26 June to 28 August 2011		9.0	Sun et al. (2012)
	March 2005 to February 2006		15.8	Yang et al. (2011)
Nanjing (32.0°N, 118.8°E)	February 2001		14.0	Yang et al. (2005)
	September 2001		11.5	Yang et al. (2005)
	15–22 February 2001		13.73	Wang et al. (2002)
Hangzhou (30.2°N, 120.1°E)	September 2001 to August 2002	Spring	15.88	Cao et al. (2009)
		Summer	14.21	Cao et al. (2009)
		Autumn	22.81	Cao et al. (2009)
		Winter	21.64	Cao et al. (2009)
Shanghai (31.2°N, 121.5°E)	20 March 1999 to 27 March 2000	Spring	12.60	Ye et al. (2003)
		Summer	10.01	Ye et al. (2003)
		Autumn	13.55	Ye et al. (2003)
		Winter	17.78	Ye et al. (2003)
	15 July to 16 August 2004		5.43	Wang et al. (2006b)
	March 1999 to May 2000		13.00	Yang et al. (2011)
Hong Kong (22.3°N, 114.2°E)	November 2000 to February 2001 and June to August 2001		8.10	Ho et al. (2006)
Xi' an (34.3°N, 108.9°E)	1996–97	Spring	59	Zhang et al. (2002)
		Summer	27	Zhang et al. (2002)
		Autumn	100	Zhang et al. (2002)
		Winter	340	Zhang et al. (2002)
	2006–07	Annual	46.7	Zhang et al. (2012c)
Qingdao (36.5°N, 121°E)	25 February to 15 March 2002		11.9	Takami et al. (2006)
	17 February to 2 March 2001		19.1	Takami et al. (2006)
Fenghuanshan (40.5°N, 124°E)	17 February to 1 March 2001		14.7	Takami et al. (2006)
Dalian (39°N, 121.5°E)	25 February to 16 March 2002		12.9	Takami et al. (2006)
	2006–07		23.3	Zhang et al. (2012c)
Lin' an (31.3°N, 120.4°E)	February–April 2001		17.3	Wang et al. (2004b)
	2006–07		21.7	Zhang et al. (2012c)
Chongqing (29.4°N, 106.3°E)	March 2005 to February 2006		25.6	Yang et al. (2011)
Guangzhou (23.1°N, 113.1°E)	31 December 2007 to 12 January 2008		8.27	Tang et al. (2009)
	December 2008 to February 2009		5.6	Yang et al. (2011)
Fuzhou (26.1°N, 119.3°E)	April 2007 to January 2008	Spring	10.14	Xu et al. (2012)
		Summer	6.62	Xu et al. (2012)
		Autumn	11.59	Xu et al. (2012)
		Winter	14.78	Xu et al. (2012)
Panyu (23.0°N, 113.4°E)	Annual 2006–07		26.8	Zhang et al. (2012c)
Zhengzhou (34.8°N, 113.7°E)			45.0	Zhang et al. (2012c)
Chengdu (30.7°N, 104°E)			40.5	Zhang et al. (2012c)
Gucheng (39.1°N, 115.8°E)			35.5	Zhang et al. (2012c)
Nanning (22.7°N, 108.4°E)			21.6	Zhang et al. (2012c)
Changde (29.2°N, 111.7°E)			28.8	Zhang et al. (2012c)
Longfengshan (44.7°N, 127.6°E)			10.0	Zhang et al. (2012c)
Dunhuang (40.2°N, 94.7°E)			6.6	Zhang et al. (2012c)
Jinsha (29.6°N, 114.2°E)			26.6	Zhang et al. (2012c)
Lhasa (29.71°N, 91.1°E)			2.9	Zhang et al. (2012c)
Gaolanshan (36.0°N, 105.9°E)			16.7	Zhang et al. (2012c)
Jinsha (29.6°N, 114.2°E)	March 2012–March 2013	Spring	12.4	Zhang et al. (2014)
		Summer	9.9	Zhang et al. (2014)
		Autumn	11.7	Zhang et al. (2014)
		Winter	16.7	Zhang et al. (2014)

Table 4. Observed concentrations of nitrate aerosol in China.

Location	Period		Concentration (μg m^{-3})	Reference
Beijing (39.9°N, 116.4°E)	July 1999 to September 2000	Summer	4.59	He et al. (2001)
		Autumn	11.16	He et al. (2001)
		Winter	15.35	He et al. (2001)
		Spring	7.26	He et al. (2001)
	2001–03	Spring	11.92	Wang et al. (2005b)
		Summer	11.18	Wang et al. (2005b)
		Autumn	9.14	Wang et al. (2005b)
		Winter	12.29	Wang et al. (2005b)
	23 January to 14 February 2007		8.38	Ianniello et al. (2011)
	2–31 August 2007		9.62	Ianniello et al. (2011)
	26 June to 28 August 2011		12.4	Sun et al. (2012)
	March 2005 to February 2006		10.1	Yang et al. (2011)
Nanjing (32.0°N, 118.8°E)	2001	February	8.06	Yang et al. (2005)
		September	3.24	Yang et al. (2005)
Hangzhou (30.2°N, 120.1°E)	September 2001 to August 2002	Spring	7.20	Cao et al. (2009)
		Summer	4.68	Cao et al. (2009)
		Autumn	7.07	Cao et al. (2009)
		Winter	11.19	Cao et al. (2009)
Shanghai (31.2°N, 121.5°E)	20 March 1999 to 27 March 2000	Spring	5.4	Ye et al. (2003)
		Summer	2.92	Ye et al. (2003)
		Autumn	5.12	Ye et al. (2003)
		Winter	9.64	Ye et al. (2003)
	March 1999 to May 2000		5.78	Yang et al. (2011)
Hong Kong (22.3°N, 114.2°E)	November 2000 to February 2001		1.20	Ho et al. (2006)
Yulin (38.20°N, 109.43°E)	30 March to 1 May 2001		1.3	Xu et al. (2004)
Xi' an (34.3°N, 108.9°E)	1996–97	Spring	33	Zhang et al. (2002)
		Summer	16	Zhang et al. (2002)
		Autumn	22	Zhang et al. (2002)
		Winter	65	Zhang et al. (2002)
	2006–07, annual		20.7	Zhang et al. (2012c)
Chongqing (29.4°N, 106.3°E)	March 2005 to February 2006		5.46	Yang et al. (2011)
Qingdao (36.5°N, 121°E)	25 February to 15 March 2002		10.3	Takami et al. (2006)
	17 February to 2 March 2001		12.5	Takami et al. (2006)
Fenghuanshan (40.5°N, 124°E)	17 February to 1 March 2001		7.3	Takami et al. (2006)
Dalian (39°N, 121.5°E)	25 February to 16 March 2002		12.8	Takami et al. (2006)
	2006–07, annual		13.5	Zhang et al. (2012c)
Lin' an (31.3°N, 120.4°E)	2006–07, annual		8.6	Zhang et al. (2012c)
Guangzhou (23.1°N, 113.1°E)	31 December 2007 to 12 January 2008		4.68	Tang et al. (2009)
	December 2008 to February 2009		12.0	Yang et al. (2011)
Fuzhou (26.1°N, 119.3°E)	April 2007 to January 2008	Spring	4.60 μ	Xu et al. (2012)
		Summer	1.10	Xu et al. (2012)
		Autumn	3.13	Xu et al. (2012)
		Winter	8.77	Xu et al. (2012)
Panyu (23.0°N, 113.4°E)	2006–07		11.7	Zhang et al. (2012c)
Zhengzhou (34.8°N, 113.7°E)			22.6	Zhang et al. (2012c)
Chengdu (30.7°N, 104°E)			15.1	Zhang et al. (2012c)
Gucheng (39.1°N, 115.8°E)			20.0	Zhang et al. (2012c)
Nanning (22.7°N, 108.4°E)			5.1	Zhang et al. (2012c)
Changde (29.2°N, 111.7°E)			8.5	Zhang et al. (2012c)
Longfengshan (44.7°N, 127.6°E)			4.9	Zhang et al. (2012c)
Dunhuang (40.2°N, 94.7°E)			2.3	Zhang et al. (2012c)
Jinsha (29.6°N, 114.2°E)			7.2	Zhang et al. (2012c)
Lhasa (29.71°N, 91.1°E)			2.3	Zhang et al. (2012c)
Gaolanshan (36.0°N, 105.9°E)			18.4	Zhang et al. (2012c)
Jinsha (29.6°N, 114.2°E)	March 2012–March 2013	Spring	3.0	Zhang et al. (2014)
		Summer	1.5	Zhang et al. (2014)
		Autumn	4.7	Zhang et al. (2014)
		Winter	9.6	Zhang et al. (2014)

largely to the $PM_{2.5}$ mass in China. Nitrate aerosol concentrations have been observed to exceed 10 μg m^{-3} in many places in winter.

In addition to anthropogenic aerosols, arid and semiarid regions in northern and northwestern China are large sources of mineral dust aerosol. Dust storms occur frequently in China in spring of every year (Zhang et al., 2003), which have large impacts on $PM_{2.5}$ concentrations over the source regions and along the transport pathway of the dust storms. For example, aerosol samples of $PM_{2.5}$ collected over 38 consecutive days in March and April of 2001 in Beijing showed that the average $PM_{2.5}$ mineral dust concentration was 14.6 μg m^{-3} during the observation period, with high $PM_{2.5}$ mineral dust concentrations of 62.4 μg m^{-3} and 54.1 μg m^{-3} on the sand-dust event days of 21 March and 10 April, respectively (Zhang et al., 2003). During a dust storm event from 21 to 26 March 2001, the total soil dust concentration (fine mode plus coarse mode) was, on average, 251.8 μg m^{-3}, which was much higher than the average value of 52.1 μg m^{-3} measured on non-dust-storm days (Zhang et al., 2008). Dust concentrations depend on wind velocity, soil moisture, and precipitation in dust sources regions as well as the deposition during transport.

4. Measured optical properties of aerosols

4.1. *Aerosol optical depth*

The spatial and temporal distributions of aerosol optical properties are the key parameters that determine the climatic effect of aerosols. The Moderate Resolution Imaging Spectrometer (MODIS) products of AOD are available since 2001. Figure 3 shows the MODIS seasonal mean distributions of aerosol optical depth over China that are averaged over years 2001–10. The highest AOD values of 0.7–1.0 were found over a large fraction of eastern China in spring, because dust storms occur in spring of every year. Throughout the year, AODs exceeding 0.5 were located over the four heavily polluted areas (northern China, the Sichuan Basin, the Yangtze River Delta, and the Pearl River Delta). Although measured aerosol concentrations are generally higher in winter than in summer (Table 2), AODs were found to be higher in summer than in winter because of the high relative humidity and hence the large water uptake by aerosols in summer.

Ground-based sunphotometric measurements are also available for understanding the columnar optical properties over China. The Chinese Sun Hazemeter Network (CSHN), launched in July 2004 by the Institute of Atmospheric Physics, Chinese Academy of Sciences, and the University of Maryland, has an extensive coverage in China (Xin et al., 2006). Based on CSHN measurements, annual mean and seasonal variations in aerosol optical properties at both urban and remote sites have been examined (Xin et al., 2007). Annual mean AOD ranges from 0.14 at clean sites to 0.7–0.9 in southeastern China (Xin et al., 2007). Du et al. (2008) compared aerosol optical properties in March to May of 2005–07 in dust and non-dust weather conditions. They found that the AOD averaged over 15 sites (including dust-source, near-source, and distant sites) increased by 33% in the presence of dust as compared to nondust conditions.

Fig. 3. MODIS seasonal mean distributions of aerosol optical depth over China that are averaged over years 2001–10: (a) December–January–February (DJF); (b) March–May–April (MAM); (c) June–July–August (JJA); (d) September–October–November (SON). MODIS datasets are level 3 products downloaded from http://ladsweb.nascom.nasa.gov.

With the establishment of Aerosol Robotic Network (AERONET) sites in China in the past decade, daily and seasonal variations in AOD have been observed at about 25 stations in China. The AOD values range from about 4 in heavily polluted episodes to about 0.2 in relatively clean conditions in northern China (Xia et al., 2006; Li et al., 2007a). Among the AERONET sites in China, only 7 sites have measurements of 5 years or longer. Since climate is measure of the average pattern of meteorological parameters in a given region, nationwide long term measurements are essential for understanding climatic effect of aerosols in China.

4.2. *Single scattering albedo*

The SSA, the ratio of aerosol scattering coefficient to extinction coefficient, is an important optical parameter that determines whether aerosols have a cooling or a warming effect. Ramanathan et al. (2001) reported that an SSA exceeding 0.95 leads to a negative aerosol forcing at the top of the atmosphere (TOA) and an SSA less than 0.85 leads to a positive forcing. Bergin et al. (2001) reported that the values of SSA were about 0.81 in northern China. Lee et al. (2007) presented a horizontal distribution of SSA values in China considering both ground-based spectral transmittance and spaceborne TOA reflectance. They found that the average of SSA values over China was 0.89 ± 0.04 at 500 nm in year 2005. More ground-based SSA measurements in China are listed in Table 5. The large differences in SSA result from the differences in chemical composition, size, shape, and hydroscopic growth of aerosol particles.

Observations show that SSA values are smaller in winter (Qiu and Yang, 2008). Increases in BC emissions might have led to the decreases in SSA in Beijing during 1993–2001 (Qiu et al., 2004). Recently, Lyapustin et al. (2011) analyzed AODs in Beijing from both AERONET measurements and MODIS retrievals, and reported an increasing trend in SSA in Beijing during 2007–10 relative to the previous five years. In addition, mineral dust aerosol can influence SSA in China. As dust particles are mixed with anthropogenic aerosols during transport, SSA values generally show increases (Xia et al., 2005).

5. Correlations between air pollutants and observed changes in meteorological parameters in China

5.1. *Reductions in atmospheric visibility*

The absorption and scattering of aerosols have large impacts on atmospheric visibility. Che et al. (2007) analyzed the observed visibility at 615 synoptic weather stations in China during 1957–2005 and found that the horizontal visibility averaged over all the stations had a large decreasing trend of -2.1 km $(10 \text{ yr})^{-1}$ after 1990. Che et al. (2007) also showed that maximum reductions in visibility correlated well with the locations of the highest concentrations of air pollutants. Deng et al. (2008) found that low visibility days in Guangzhou occurred rarely (less than a few days per year) during 1954–72,

but were about 150 days per year during 1980–2006. Wang et al. (2009) estimated the changes in AOD and atmospheric visibility by using the National Climatic Data Center Global Summary of Day datasets collected from about 3250 meteorological stations from 1973 to 2007. They found that AOD values over land have been increasing on a global mean basis, with large increases in AOD and hence significant reductions in visibility in eastern China.

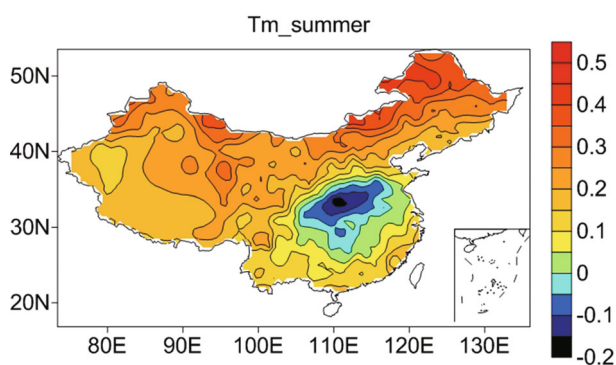### 5.2. *Reductions in solar radiation at the surface*

The impacts of absorption and scattering by aerosols can also be seen in changes of solar radiation at the surface (Li et al., 2011a; Xu et al., 2011). Analysis of data from about 200 meteorological observing stations showed significant decreases in sunshine duration over a large fraction of China [approximately 1% $(10 \text{ yr})^{-1}$ averaged over the whole China] for the period 1954–98 (Kaiser and Qian, 2002). The sunshine duration was measured by a sunshine recorder, expressed to the nearest 0.1 h, in which the direct solar radiation was of sufficient intensity to activate the recorder (a rough approximation of the amount of energy in the direct beam necessary to activate the recorder is 0.12 cal cm^{-2} min^{-1}). Zheng et al. (2008) obtained similar results by analyzing observations at 184 weather stations across the Yunnan-Guizhou Plateau (YGP) in southwestern China for the years 1961–2005. It was found that over this 45-year period annual sunshine duration decreased largely in the northern YGP (north of 24°N), with negative trends reaching -11.8% $(10 \text{ yr})^{-1}$. Increases of aerosols in the atmosphere were found to be responsible for the changes in clear-sky global and direct radiation (Liang and Xia, 2005; Qian et al., 2007). Over the second half of the 20th century, while there were significant decreases in global radiation [-4.5 W m^{-2} $(10 \text{ yr})^{-1}$], direct radiation [-6.6 W m^{-2} $(10 \text{ yr})^{-1}$], and sunshine duration [-1.28% $(10 \text{ yr})^{-1}$], the diffuse fraction exhibited increases [1.73% $(10 \text{ yr})^{-1}$] as a result of aerosol scattering (Che et al., 2005).

5.3. *Changes in surface air temperature*

Changes in solar radiation at the surface are expected to lead to changes in surface temperature. Along with global warming, the annual mean surface air temperature averaged over China has increased over recent decades (Wang et al., 2004a; Cao et al., 2013). However, the changes in summer temperature over the period 1960–2008 showed that a negative summer temperature trend of up to $-0.2°C$ $(10 \text{ yr})^{-1}$ existed in the Yangtze–Huaihe basins and a warming occurred in northern China and the western provinces (Fig. 4). Several studies attempted to explain the decreases in summer temperature in the Yangtze–Huaihe basins by the increases in aerosols in these regions. Kaiser and Qian (2002) found a significant decrease in summertime maximum temperature over the period 1954–98 near the Sichuan Basin, where the largest AOD and decreases in sunshine duration occurred. Shi et al. (2008), by examining the distributions and variations of surface air temperature and Total Ozone Mapping Spectrometer (TOMS) AOD in March to August of 1979–2000 over

Table 5. Ground-based aerosol single scattering albedo in China.

Location	Period	Single scattering albedo	Reference
Beijing	June 1999	0.81 ± 0.08	Bergin et al. (2001); relative humidity $< 40\%$
	1993–2001	0.84 (550 nm)	Qiu et al. (2004)
	January 2005	0.78 ± 0.11 (532 nm)	Muller et al. (2006)
	2002–07	0.89 (spring)	Yu et al. (2009); average SSA at wavelengths of 440, 675, 870, and 1020 nm
		0.91 (summer)	Yu et al. (2009); average SSA at wavelengths of 440, 675, 870, and 1020 nm
		0.87 (autumn)	Yu et al. (2009); average SSA at wavelengths of 440, 675, 870, and 1020 nm
		0.86 (winter)	Yu et al. (2009); average SSA at wavelengths of 440, 675, 870, and 1020 nm
	2005–06	0.80 ± 0.09 (525 nm)	He et al. (2009); relative humidity $< 60\%$
	11 August to 6 September 2006	0.86 ± 0.07 (535 nm)	Garland et al. (2009); relative humidity $28 \pm 4\%$
	2001–04	0.9 (440 nm)	Xia et al. (2006)
	2005	0.88 (550 nm)	Lee et al. (2007)
	1998–2003	0.89 (400–1000 nm)	Qiu and Yang (2008)
Shangdianzi	September 2003 to January 2005	0.88 ± 0.05 (525 nm)	Yan et al. (2008); relative humidity $< 60\%$
Xianghe	September 2004 to September 2005	0.92 (441 nm)	Li et al. (2007a)
		0.92 (673 nm)	Li et al. (2007a)
		0.91 (873 nm)	Li et al. (2007a)
		0.91 (1022 nm)	Li et al. (2007a)
	March 2005	0.81–0.85 (550 nm)	Li et al. (2007c); relative humidity 36%
	2005	0.87 (550 nm)	Lee et al. (2007)
Harbin	1993–2001	0.85 (550 nm)	Qiu et al. (2004)
Shenyang	1993–2001	0.80 (550 nm)	Qiu et al. (2004)
	2005	0.89 (550 nm)	Lee et al. (2007)
	1998–2003	0.88 (400–1000 nm)	Qiu and Yang (2008)
Zhengzhou	1993–2001	0.85 (550 nm)	Qiu et al. (2004)
	1998–2003	0.92 (400–1000 nm)	Qiu and Yang (2008)
Wuqing	March 2009	0.82 ± 0.05 (637 nm, spring)	Ma et al. (2011); dry aerosol
	July–August 2009	0.86 ± 0.05 (637 nm, summer)	Ma et al. (2011); dry aerosol
Xinken	October 2004	0.77 ± 0.12 (532nm)	Muller et al. (2006)
	October–November, 2004	0.85 ± 0.04 (550 nm)	Wendisch et al. (2008); dry aerosol
	October 2004	0.83 ± 0.05 (550 nm)	Cheng et al. (2008); relative humidity $< 10\%$
Guangzhou	October 2004	0.83 (540 nm)	Andreae et al. (2008); relative humidity $< 45\%$
Taibei	2005	0.83 (550 nm)	Lee et al. (2007)
Shanghai	2005	0.87 (550 nm)	Lee et al. (2007)
	1998–2003	0.90 (400–1000 nm)	Qiu and Yang (2008)
Wuhan	1998–2003	0.94 (400–1000 nm)	Qiu and Yang (2008)
Linan	November 1999	0.93 ± 0.04 (530 nm)	Xu et al. (2002); relative humidity $< 40\%$
Shouxian	May–December 2008	0.92 (550 nm)	Fan et al. (2010); relative humidity $< 40\%$
Dunhuang	1998–2000	0.90 (500 nm)	Kim et al. (2004)
Yinchuan	1998–2000	0.91 (500 nm)	Kim et al. (2004)
	October 2003 to August 2004	0.83–0.95 (500 nm)	Liu et al. (2008)
Yulin	April 2001	0.95 ± 0.05	Xu et al. (2004); relative humidity $35 \pm 21\%$
Ürümqi	1993–2001	0.84 (550 nm)	Qiu et al. (2004)
	1998–2003	0.89 (400–1000 nm)	Qiu and Yang (2008)
Lanzhou	1993–2001	0.81 (550 nm)	Qiu et al. (2004)
	2005	0.89 (550 nm)	Lee et al. (2007)
	1998–2003	0.85 (400–1000 nm)	Qiu and Yang (2008)
Chengdu	1998–2003	0.90 (400–1000 nm)	Qiu and Yang (2008)

Fig. 4. Trends in summer (JJA) mean temperature [unit: $K\ (10\ yr)^{-1}$] for the period 1960–2008. The datasets of homogenized daily mean temperatures at 549 National Standard Stations in China for 1960–2008 are taken from Li and Yan (2009).

eastern China, found that AOD and surface air temperature were negatively correlated. A similar negative correlation between the increases in AOD and reductions in temperature in eastern China in the past 50 years has also been reported in Chen et al. (2009).

5.4. *Changes in precipitation and clouds*

The radiative effect of aerosols can influence precipitation in a number of ways. The direct effect of aerosols reduces surface temperature, evaporation, and atmospheric stability, which can lead to reductions in precipitation (Zhao et al., 2006; Duan and Mao, 2008). Aerosol-induced increases in cloud condensation nuclei (CCN) lead to increased cloud droplet concentrations and smaller droplets, which can have an effect of reducing precipitation (Twomey, 1959, 1977; Albrecht, 1989). Hansen et al. (1997) and Ackerman et al. (2000) identified a so-called "semi-direct" effect, in which changes in the thermal structure of the atmosphere resulting from aerosol solar absorption (principally by BC) suppress cloud formation/precipitation. Furthermore, aerosol-induced changes in temperature gradient can influence atmospheric circulation and hence atmospheric water vapor supply.

Precipitation in eastern China is associated with the Asian summer monsoon. Every year, the rain belts of summer monsoon appear firstly over southern China from April to mid-June, intensify and shift to the middle and lower reaches of the Yangtze River around mid-June, and then move to northern China in mid-July and last until mid-August. Zhao et al. (2006) examined observed precipitation, MODIS AOD, and meteorological sounding datasets over northern China, and found that precipitation in this region was significantly reduced during 1961–2000 (the decreasing trend at some stations was larger than 0.4% yr^{-1}). This reduction in precipitation was found to correlate with high concentrations of aerosols and was explained by a positive feedback mechanism. The aerosol-induced enhancement in atmospheric stability depresses upward motion and precipitation, further increasing aerosol concentrations. They found that the percentage of unstable days in northern China was approxi-

mately 34% during the late 1980s, and then about 17% in the 2000s. Qian et al. (2009) reported that both the frequency and amount of observed light rain (events or days with precipitation less than either 2 mm or 5 mm) decreased in the whole of eastern China over 1956–2005 as a result of the aerosol indirect effect. This trend for light rain is different from that of total rainfall observed in eastern China, which shows decreases in northern China and increases in southeastern China. Choi et al. (2008) also showed that, over recent decades, increases in aerosol concentrations correlated negatively with the trend in light rain ($< 5\ mm\ d^{-1}$) and positively with changes in moderate rainfall (10–$20\ mm\ d^{-1}$) in China. A study by Rosenfeld et al. (2008) proposed that interactions of aerosols with deep convective clouds could increase precipitation, which might be responsible for the observed increases in precipitation in southern China where aerosol concentrations were high and water vapor supply was adequate.

With respect to changes in clouds, Shi et al. (2008) showed a positive correlation between increases in AOD and those in low clouds in southern China in the past two decades. Bennartz et al. (2011) reported that cloud droplet number concentrations, derived from the Patmos-x satellite observations over the East China Sea downwind of emission sources, increased from less than $200\ cm^{-3}$ in the 1980s to more than $300\ cm^{-3}$ in 2005. Zhang et al. (2011) studied the effect of aerosols on clouds in Beijing based on *in situ* aircraft measurements during the period of July to September in 2008. Higher aerosol concentrations were observed to lead to a larger number of cloud droplets with smaller size. The activation of aerosol particles to become cloud droplets was significantly enhanced with liquid water content (LWC) exceeding $0.5\ g\ m^{-3}$. However, Tang et al. (2014) found positive correlations between water cloud effective radius (CER) and AOD over eastern China by using MODIS retrievals for 2003–13. Their analysis for North China Plain showed that variations in wind speed and relative humidity might have caused the positive correlations. Southerly winds carry high levels of aerosols and abundant water vapor, resulting in coincident increases in both AOD and CER in North China Plain, while the northerly winds transport dry and clean air from high latitudes, leading to decreases in AOD and CER (Tang et al., 2014). The uncertainties with correlations between AOD and CER indicate the uniqueness of aerosol-cloud interactions in China and also call for further observational and modeling studies.

6. Radiative forcing

6.1. *Radiative forcing by tropospheric ozone*

Few studies have examined the radiative forcing by tropospheric O_3 over China. Wang et al. (2005a) estimated the forcing over the Chinese domain using a coupled regional chemistry–climate model (RegCM2). They found that, at the tropopause, tropospheric O_3 has a shortwave forcing of $0.19\ W\ m^{-2}$ and a longwave forcing of $0.46\ W\ m^{-2}$. The normalized net radiative forcing over China was found to be

0.02 W m^{-2} DU^{-1}, which was lower than the global mean values of 0.03–0.05 W m^{-2} DU^{-1} reported in the literature (Wang et al., 2005a). Chang and Liao (2009) estimated the anthropogenic radiative forcing by tropospheric O$_3$ based on the IPCC AR5 emissions inventories; the tropopause forcing (shortwave plus longwave) averaged over eastern China ($95°$–$125°$E, $18°$–$45°$N) was found to be 0.53 W m^{-2}.

6.2. *Direct radiative forcing by aerosols*

For the calculation of aerosol direct radiative forcing, the optical parameters used in the radiative transfer module of climate models are AOD, SSA, and asymmetry factor. These optical properties are dependent of the concentrations, size, and hygroscopic growth of aerosols. Earlier studies quantified the radiative forcing by a single aerosol species. Giorgi et al. (2002) performed a coupled climate–chemistry/aerosol simulation for China for the period 1993–97. Over eastern China, anthropogenic sulfate was found to induce a negative TOA radiative forcing that varied spatially from -1 to -8 W m^{-2} in winter and from -1 to -15 W m^{-2} in summer. Fossil fuel BC was estimated to exert a positive TOA radiative forcing of 0.5–2 W m^{-2} (Giorgi et al., 2002). Recently, direct radiative forcing by BC in China was estimated by Wu et al. (2008) and Zhuang et al. (2011; 2013), and that by nitrate was calculated by Wang et al. (2010), Zhang et al. (2012a), and Li et al. (2014).

With more advanced models that can simulate multiple aerosol species, recent studies have estimated aerosol forcing by mixed aerosol species. Qian et al. (2003) used the offline concentrations of sulfate, OC, BC, mineral dust, and sea salt from a global transport model in the Penn State/NCAR Mesoscale Model MM5 to examine the aerosol direct effect. The direct radiative forcing of aerosols in eastern China (east of $100°$E) was found to be in the range of -1 to -14 W m^{-2} in autumn and summer, and -1 to -9 W m^{-2} in spring and winter. The annual radiative forcing in eastern China ($110°$–$120°$E, $21°$–$37°$N) was estimated to be -5.11 W m^{-2} (Qian et al., 2003). Han (2010), by using the Regional Integrated Environmental Model System (RIEMS), simulated the direct radiative effect of externally mixed sulfate, BC, OC, soil dust, and sea salt aerosols over East Asia ($75°$–$145°$E, $15°$–$55°$N). They showed that the direct radiative effect of aerosols had apparent seasonal variations (Fig. 5). Averaged over East Asia, the annual mean direct radiative effect under all-sky condition was calculated to be -6.2 W m^{-2} at the surface and -0.2 W m^{-2} at the TOA (Han, 2010).

Chang and Liao (2009) estimated the anthropogenic radiative forcing of sulfate, nitrate, BC, OC, and the internal mixture of all these species by using a general circulation model with online simulations of gas-phase chemistry and aerosols. The radiative forcing values averaged over eastern China ($95°$–$125°$E, $18°$–$45°$N) are shown in Table 6. Based on the IPCC AR5 emissions inventories, the simulated annual mean anthropogenic radiative forcings by sulfate, nitrate, BC, OC, and the internal mixture of these aerosols were, respectively, -2.50, -0.75, 0.58, -0.13, and -2.40 W m^{-2} at the TOA, and -2.55, -0.77, -1.50, -0.25, and -5.40 W m^{-2}

at the surface. The annual mean maximum cooling over eastern China was predicted to exceed -6 W m^{-2} at the TOA and be up to -13 W m^{-2} at the surface.
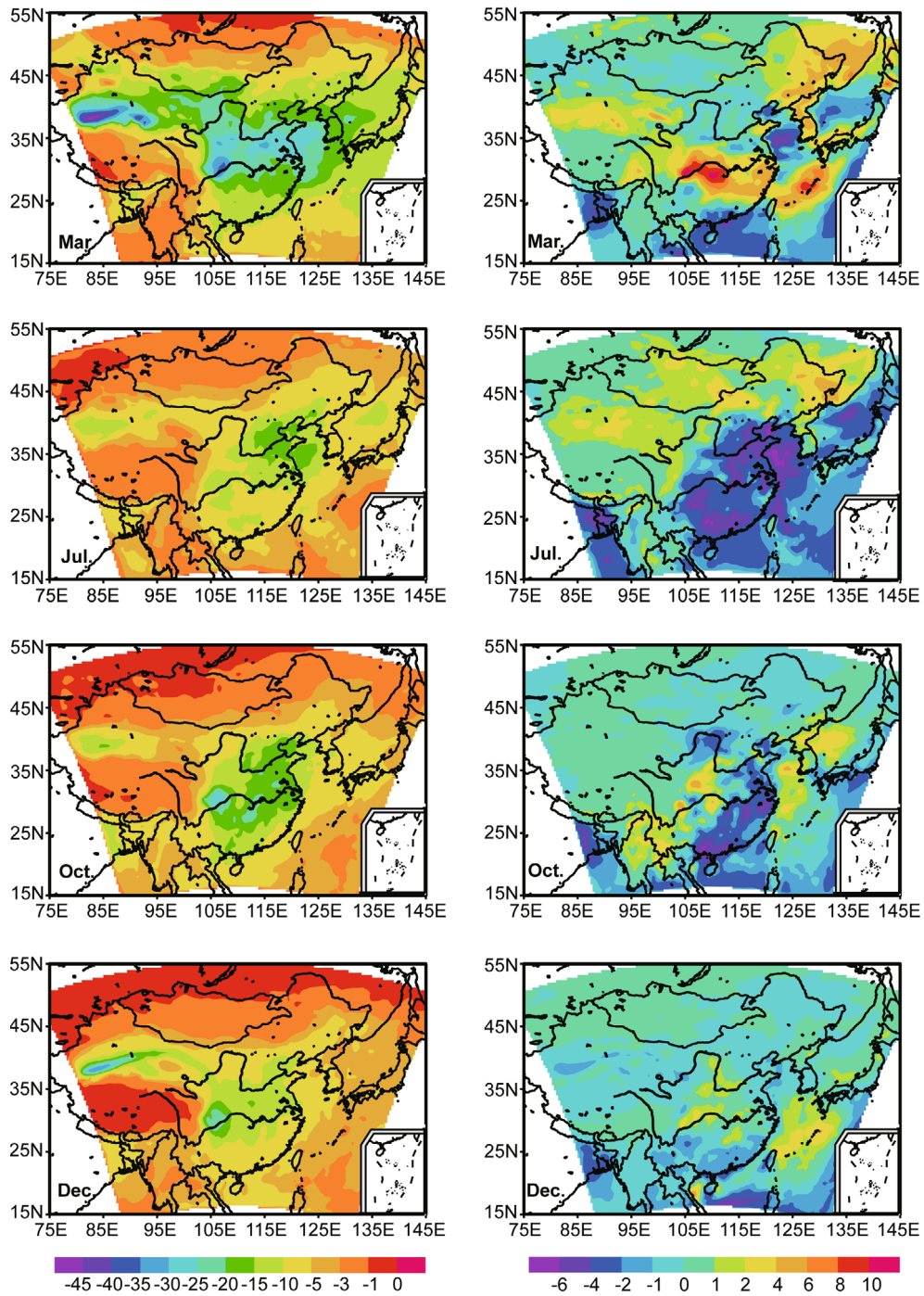
Some studies have also estimated forcing based on ground or satellite observations of AOD and solar irradiance (Li et al., 2007c; Xia et al., 2007a, b). Aerosol-induced reduction in surface shortwave irradiance was estimated to be about 30 W m^{-2} at Liaozhong in northeastern China during April to June of 2005 (Xia et al., 2007a). At Xianghe near Beijing, the annual and daily (24 h) mean aerosol radiative effect at the surface (24 W m^{-2}) was only moderately lower than the cloud radiative effect (41 W m^{-2}) (Li et al., 2007c). It should be noted that studies based on measurements usually obtained clear-sky radiative forcing by both natural and anthropogenic aerosols (i.e., they could not obtain cloudy-sky forcing and could not separate the effect of a specific aerosol species).

The high direct radiative forcing values by aerosols indicate their important roles in climate change. The estimated forcing values over China differ largely, because of the differences in emissions inventories, chemistry scheme, model year or month, and the different aerosol species considered.

6.3. *Indirect radiative forcing by aerosols*

Estimated indirect forcing values are usually dependent on the treatment of aerosol effects on cloud microphysics in climate models. Previous studies usually used one of the following two approaches in the calculation of cloud droplet number concentrations: (1) the empirical correlations between aerosol mass and cloud number concentrations obtained based on measurements (e.g., Boucher and Lohmann, 1995); and (2) first-principle approaches (e.g., Ghan et al., 1997), which simulate cloud droplet number balance in each GCM grid cell, including processes such as the activation of aerosol into cloud droplets, evaporation and collision/coalescence affecting droplet number concentrations. Because of the lack of measurements in China, empirical correlations between aerosol mass and cloud number concentrations used in the first approach are generally parameterized based on measurements in Europe or the U.S., which may not be representative of aerosol–cloud interactions in China.

Giorgi et al. (2003) reported the regionally averaged TOA indirect radiative forcing due to sulfate and BC aerosols. While the direct radiative forcing showed a weak seasonal cycle (seasonal mean TOA direct forcing values ranged from -2.29 W m^{-2} to -2.74 W m^{-2} over eastern China), the total of direct and indirect forcing showed a very strong seasonal variation [the total negative TOA radiative forcing varied from -3.93 W m^{-2} in December–January–February (DJF) to -11.77 W m^{-2} in June–July–August (JJA) over eastern China]. The indirect forcing was found to dominate in the warm and wet seasons of March–April–May (MAM) and JJA, when the cloud amount is the largest in a year. Huang et al. (2006) considered sulfate, BC, and OC aerosols in their simulations. Averaged over eastern China, the direct and first indirect effects were predicted to produce a negative net radiative forcing of -4.6 W m^{-2} at the TOA, and the sec-

Fig. 5. Simulated all-sky aerosol direct radiative effect (W m^{-2}) at the surface (left column) and at the TOA (right column) for March, July, October, and December of year 2006. [Reprinted from Fig. 6 in Han (2010).]

ond indirect effect was predicted to generate a negative net forcing of approximately -3.2 W m^{-2} at the TOA. Huang et al. (2007) reported the surface-layer seasonal mean radiative forcing by sulfate and OC aerosols in eastern China; the forcing was found to be -1.3 to -2.3 W m^{-2} as a result of direct scattering, and the value was predicted to be -4.2 to -9.6 W m^{-2} with the combined direct, semidirect, and first indirect effects. The maximum surface forcing was found to

reach -30 W m^{-2} in the areas with high aerosol concentrations.

Because of the high nitrate aerosol concentrations in China (Table 4), it is of interest to estimate radiative forcing by nitrate aerosol. Wang et al. (2010) used the RegCM3 model coupled with chemistry and aerosol schemes to calculate direct and indirect effects of nitrate aerosol in China. They reported that nitrate indirect radiative forcing is higher

Table 6. Predicted annual mean global burdens (Tg yr^{-1}) of aerosols and O$_3$ in 1850 and 2000, as well as the estimated radiative forcings (RF) (W m^{-2}) at the top of the atmosphere (TOA) and surface (SRF). Ozone forcing is also given at the tropopause*. Forcing values are averaged over the globe or over eastern China (18°–45°N, 95°–125°E) (Chang et al., 2009).

		1850	2000	RF (global)		RF (eastern China*)	
				TOA	SRF	TOA	SRF
SO$_4^{2-}$		0.79	1.90	−0.56	−0.56	−2.50	−2.55
NO$_3^-$		0.35	0.90	−0.26	−0.26	−0.75	−0.77
BC		0.05	0.11	0.13	−0.25	0.58	−1.50
OC	POA	0.49	0.71	−0.02	−0.05	−0.13	−0.25
	SOA	0.34	0.32				
All aerosol				−0.60	−1.20	−2.40	−5.40
Tropospheric O$_3$		269	377	0.17	0.05	0.24	0.09
			0.39*		0.53*		

than its direct radiative forcing; the annual mean direct radiative and first indirect radiative forcings at the TOA were estimated to be −0.88 W m^{-2} and −2.47 W m^{-2}, respectively, as forcings were averaged over the whole of China.

The indirect effects of aerosols on solar radiation found in these studies were qualitatively similar to other reports in the literature; increases in cloudiness and small cloud droplets enhance the scattering of solar radiation. The impacts of such changes in cloud properties on solar radiation are still uncertain; more physical-based methods to determine cloud droplet concentrations from aerosol concentrations and other relevant parameters should be the subject of future studies on aerosol indirect effects in China.

6.4. *Comparisons with IPCC global mean forcing values*

The tropopause forcing by tropospheric O$_3$ in eastern China was estimated by Wang et al. (2005a) and Chang and Liao (2009) to be 0.53–0.65 W m^{-2}, which are close to the high end of the global mean values of 0.40 (0.20 to 0.60) W m^{-2} estimated in IPCC AR5. Radiative forcings of aerosols in China are much higher than the global mean direct radiative forcing of −0.45 (−0.95 to 0.05) W m^{-2} and indirect radiative forcing of −0.45 (−1.2 to 0.0) W m^{-2} reported in IPCC AR5. Radiative forcing by aerosols in China is also much stronger than the global mean radiative forcing of 2.83 (2.26 to 3.40) W m^{-2} by the increases in CO$_2$, CH$_4$, N$_2$O, and halocarbons from preindustrial times. These high radiative forcing values indicate that air pollutants in China can have important roles in regional and global climate change.

7. Simulated climatic effects of air pollutants

To understand the roles of air pollutants in climate change in China, it is important to have a clear picture of climate change in China over the past several decades. While a warming was observed in China on an annual mean basis (Cao et al., 2013), a negative summer temperature trend existed in the Yangtze–Huaihe basins (Fig. 4). The observed changes in precipitation over the past decades showed that summer precipitation decreased in northern and southeastern China and increased in the Yangtze Basin (Xu, 2001). Climate change

in China is associated with changes in the East Asian monsoon. According to the monsoon index defined by Li and Zeng (2002, 2003, 2005), the East Asian summer monsoon has been weakening since 1950. A strong summer monsoon is characterized by strong southerlies extending from southern to northern China, a deficit of rainfall in the middle and lower reaches of the Yangtze River, and high rainfall in northern China (Li and Zeng, 2002; Wang et al., 2008). On the contrary, a weak summer monsoon in China features weak southerlies that cannot push the monsoon system far enough northward, resulting in high rainfall in southern China and a deficit of rainfall in northern China. These changes in the Asian summer monsoon can help to explain the observed changes in summer temperature and precipitation, but the roles of air pollutants need to be quantified.

The climatic effects of air pollutants (either tropospheric O$_3$ or aerosols) in China have been examined by some regional or global climate models. Regional climate models have the advantage of high spatial and temporal resolutions, but they cannot account for changes in large-scale circulation if the regional climate simulations with or without air pollutants use the same boundary conditions. Although forcings by air pollutants are quite regional, they can influence large-scale circulation by altering temperature gradients; climate responses to the forcings are not local, as demonstrated by many global studies. Global simulations of climatic effects of air pollutants usually take one of two forms: (1) equilibrium climate, in which the long-term climate that would result from a fixed pollutant concentration is computed; and (2) transient climate, in which climate is simulated from a starting point, say preindustrial, with specified annual emissions changes. Predicted changes from an equilibrium climate simulation generally exceed those from a transient climate simulation. For example, the ratio of the transient climate response (the change in surface air temperature at the time of doubled CO$_2$) to the equilibrium response (the equilibrium change in surface air temperature from doubled CO$_2$) lies in the range of 0.47–0.68 (IPCC, 1995).

7.1. *Climatic effect of tropospheric ozone*

A few studies have examined climate change induced by tropospheric ozone in China. Wang et al. (2004b) used the

coupled regional chemistry–climate model RegCM2 (Giorgi et al., 2002) to simulate the concentrations and climatic effect of tropospheric O_3 in China. They found that the monthly mean column burden of O_3 was about 30 DU in eastern China, which led to changes in surface air temperature by −0.8 to 0.8 K. The negative changes in temperature were mainly associated with the feedback of clouds. Hansen et al. (2007) examined the climatic responses to changes in tropospheric ozone over the period 1900–2003 based on transient climate simulations with the GISS ModelE, and their predicted increases in temperature reached up to 0.5 K over eastern China. Chang et al. (2009) reported, based on a global coupled chemistry–climate simulation, that the warming due to changes in tropospheric O_3 over the period 1950–2000 was 0.43 K in eastern China (Table 7). These results indicate that it is important to consider the radiative effect of tropospheric O_3 in simulations of climate change in China.

7.2. *Climatic effect of tropospheric aerosols*

7.2.1. *Regional simulations of the climatic effect of aerosols*

Giorgi et al. (2002) performed a number of multi-year regional simulations to assess the climatic impact of anthropogenic sulfate and BC. Using anthropogenic emissions, they found that the direct effects of anthropogenic sulfate and BC can induce a surface cooling of −0.1 to −0.7 K, highly variable at the subregional scale. Qian et al. (2003), using the offline fields of sulfate, OC, BC, mineral dust, and sea salt, reported that the negative radiative forcing of aerosols was predicted to induce a surface cooling in the range of −0.6 to −1.2 K in autumn and winter, −0.3 to −0.6 K in spring and 0.0 to −0.9 K in summer throughout eastern China.

Giorgi et al. (2003) advanced the regional study by including the first indirect effect of anthropogenic sulfate. Averaging over eastern China (approximately east of 90°E and between 20°–40°N), the direct radiative effect of sulfate and soot was predicted to reduce surface air temperature by 0.07 K in JJA and 0.21 K in DJF. Such larger reduction in temperature in winter than in summer was also found by Chen et al. (2007). With the addition of the first indirect effect, the impact of sulfate and soot on surface air temperature was predicted to be about −0.4 K in all seasons. Predicted changes in precipitation in DJF, MAM, JJA, and September–October–November (SON) were, respectively, −5.9%, −2.3%, −1.7%, and −4.2%, with the direct effect of sulfate and soot, and −12.6%, −7.9%, −5.3%,

and −9.9% when both direct and first indirect effects were considered.

Huang et al. (2007) used a coupled regional chemistry–aerosol–climate model to assess the direct and indirect effects of anthropogenic sulfate and carbonaceous aerosols (OC and BC) on regional climate in East Asia. The direct and first indirect effects were simulated to reduce solar radiation and hence decrease the surface temperature in a large fraction of eastern China, with the magnitude of the simulated changes in surface air temperature compatible with the results obtained by Giorgi et al. (2003). The second indirect effect was predicted to generate both negative solar forcing and a substantial positive longwave forcing, which led to decreases in precipitation, but because of the cancellation effect, very small changes in surface temperature (Huang et al., 2007). With the interactively calculated aerosol loading and the combined direct/semidirect/first indirect radiative effects, the simulated precipitation was reduced by about 10% in autumn and winter and by about 5% in spring and summer. The second indirect effect was shown to have the largest impact on precipitation, which was predicted to reduce the precipitation in autumn and winter from about 3% to 20%, depending on the autoconversion scheme used (Huang et al., 2007). The semidirect effect on precipitation was found to be relatively small.

Long-term observational datasets reveal that both the frequency and amount of light rain decreased in eastern China during the period 1956–2005. Qian et al. (2009) showed by using a cloud-resolving model and satellite data that high concentrations of aerosols in eastern China can significantly increase cloud droplet number concentrations and reduce droplet sizes compared to pristine conditions, leading to significant reductions in raindrop concentrations and a delay in raindrop formation because smaller cloud droplets are less efficient in collision and coalescence processes. Results indicated that the significantly increased aerosol concentrations were at least partly responsible for the decreased light rain observed in China over the past 50 years.

Besides studies that have examined scattering or mixed aerosols, Wu et al. (2004, 2008) examined the climatic effect of BC alone. Using the Regional Integrated Environmental Modeling System (RIEMS) and the CCM3 radiation scheme, Wu et al. (2004) performed simulations for the months of January, April, July, and October in 2000. The radiative forcing of BC was predicted to lead to decreases in surface temperature in East Asia by 0.12–0.15 K in January, 0.25 K in April,

Table 7. Summary of the average changes of selected climate variables over the period 1950–2000 in eastern China (20°–50°N, 100°–130°E) (Chang et al., 2009).

	ΔSO4	ΔBC	ΔBCSO4	ΔBCSO4POA	ΔAER	ΔO3	ΔGHG
Temperature (°C)	−0.40	0.62	0.18	0.15	−0.78	0.43	0.85
Radiation (W m^{-2})	−1.09	−0.91	−2.71	−2.98	−7.29	0.40	1.12
Latent heat (W m^{-2})	1.92	−0.55	1.38	1.17	5.18	−0.86	−2.26
Sensible heat (W m^{-2})	−1.03	1.41	1.37	1.83	1.67	0.73	1.34
Precipitation (mm d^{-1})	−0.21	0.07	−0.03	0.02	−0.24	0.08	0.10

0.3–1.5 K in July, and 0.2–0.5 K in October. The maximum decreases in temperature were located over the Yangtze River drainage basin and southern China. Wu et al. (2008) further examined the direct effect of BC on the hydrological cycle in China using the RegCM3 model (Giorgi et al., 2002). Water vapor was predicted to increase by 0.6% in southern China but to decrease by up to 0.3% in northern China. The increases in water vapor content in southern China were mainly caused by the strengthening of airflow from the South China Sea. The radiative forcing of BC was found to lead to an increase in precipitation by 0.4–0.6 mm d^{-1} in southern China.

7.2.2.   *Equilibrium climate simulations using global models*

Menon et al. (2002) studied the equilibrium climatic responses to the direct and semidirect effect of aerosols over China and India using a global climate model with fixed SSTs. By considering anthropogenic aerosols, their simulation reproduced the observed increases in precipitation in southeast China and decreases in precipitation in northeast China. These changes in precipitation were attributable to the absorption (as opposed to the scattering) of radiation by the observed AOD distribution. Their model results were dependent on the assumed SSA value of 0.85, which was too low as compared to the observed SSA values in China (Table 5).

Gu et al. (2006) investigated the equilibrium climate responses to the direct radiative forcing of both natural and anthropogenic aerosols in China using the general circulation model developed at the University of California, Los Angeles (UCLA GCM). They assumed a global background AOD of 0.2, consisting of 90% maritime and 10% BC based on the observations of TOMS. Over the Chinese domain, observed changes in AODs were used to simulate the climatic effect of aerosols. Total cloud cover was predicted to decrease in northern and western China, which agreed with the observed decreases over the period 1951–94. Aerosols in China were predicted to lead to a cooling in the midlatitudes of the NH, strengthening the meridional circulation and then increasing precipitation in southern China. This predicted precipitation anomaly was similar to that presented by Menon et al. (2002). However, Gu et al. (2006) argued that the increased precipitation in southern China might be related to the increased AOD rather than the absorption of aerosol as suggested by Menon et al. (2002).

Kim et al. (2007) studied the equilibrium climatic effect of sulfate aerosol radiative forcing on spring rainfall in East Asia based on numerical simulations with the NASA finite-volume General Circulation Model (fvGCM). The climate simulations were forced with monthly varying three-dimensional aerosol distribution from the Goddard Ozone Chemistry Aerosol Radiation and Transport model (GO-CART). The reanalyzed weekly SSTs from September 1986 to December 1996 were interpolated to daily values. The radiative forcing of sulfate aerosol was predicted to lead to a cooling at the land surface and a reduction in rainfall over central East Asia. The maximum reduction in precipitation was found to be located to the north of the area with the max-

imum aerosol loading as a result of dynamical feedback. An anomalous thermal gradient due to aerosol cooling near the land surface can reduce the baroclinicity of the atmosphere, leading to a deceleration of the upper-level westerly flow. The westerly deceleration induces, through ageostrophic wind adjustment, anomalous meridional secondary circulation at the entrance region of the East Asian jet stream, with a strong descending flow and suppressed precipitation near 30°N, but a weak ascent of air and moderately enhanced precipitation over southern China and the South China Sea. Their results suggested that aerosol radiative forcing and the associated feedback contributed to the observed trend of spring precipitation in East Asia.

A number of recent global studies have also considered the aerosol indirect effect. Takemura et al. (2005) simulated the equilibrium climate responses to aerosol direct and indirect effects with a coupled global aerosol transport–radiation–climate model. They predicted a large reduction of about 2 K in temperature and a general reduction in precipitation over East Asia. To explain the observed decreases in precipitation in southern China (114°–120°E, 23°–27°N) in early summer over the past decades, Cheng et al. (2005) applied the ECHAM4 GCM with a fully coupled aerosol–cloud microphysics module to investigate the role of the aerosol second indirect effect by sulfate, BC, and OC in the drought of early summer in southern China. They separated the role of the aerosol second indirect effect from the roles of the increases in SSTs and greenhouse gases (GHGs). Model results showed that both the aerosol indirect effect and changes in SSTs/GHGs contributed to the observed increases in low-level cloud and decreases in precipitation over the period 1961–2000 in southern China, and the impact of the aerosol indirect effect was larger than the effect of SST/GHGs.

7.2.3.   *Transient climate simulations using global models*

Li et al. (2007b) considered the sulfate direct radiative effect in a simulation over the period 1949–2002 using a GCM. They found that sulfate aerosol can induce a positive gradient of air temperature from the middle to the upper troposphere, which results in a northward shift of the East Asian westerly jet stream at 200 hPa and a strengthening of the East Asian summer monsoon. They simulated a surface cooling of about 1 K and increases in cloud cover and precipitation in eastern China over the period 1949–2002.

Chang et al. (2009) investigated the direct climatic effects of five anthropogenic aerosols, including SO_4^{2-}, NO_3^-, BC, POA, and SOA, in eastern China over the period 1951–2000. Concentrations of SO_4^{2-}, NO_3^-, POA, SOA, BC, and tropospheric O_3 for the years 1950 and 2000 were obtained a priori by the Goddard Institute for Space Studies (GISS) GCM with coupled chemistry and aerosols, and then monthly concentrations of these species were interpolated linearly between 1951 and 2000 in transient climate simulations. BC aerosol was assumed to be internally mixed with other aerosol species in all simulations. Model results indicated that simulated changes in temperature and precipitation over 1950–2000 were very sensitive to the consideration of aerosol

species (Figs. 6 and 7). For example, the predicted sign of changes in surface air temperature by $BC + SO_4^{2-} + POA$ aerosols was different from that by all aerosol species ($BC + SO_4^{2-} + POA + SOA + NO_3^-$). They also compared the climatic effect of aerosols with the impacts of tropospheric O_3 and GHGs over eastern China (Figs. 6 and 7). As can be seen in Table 7, relative to the climate simulation without changes in GHGs, O_3, and aerosols, anthropogenic forcings of SO_4^{2-}, BC, $BC + SO_4^{2-}$, $BC + SO_4^{2-} + POA$, $BC + SO_4^{2-} + POA + SOA + NO_3^-$, O_3, and GHGs over the period 1950–2000 were predicted to change surface air temperature in eastern China ($100°$–$130°E$, $20°$–$50°N$), respectively, by $-0.40°C$, $0.62°C$, $0.18°C$, $0.15°C$, $-0.78°C$, $0.43°C$, and $0.85°C$, and to change precipitation averaged over the same domain, respectively, by -0.21, 0.07, -0.03, 0.02, -0.24, -0.08, and 0.10 mm d^{-1}. They concluded that aerosols, when all major aerosol species are considered, are as important as GHGs in influencing climate change in eastern China.

7.2.4. *Uncertainties with simulated climatic effect of aerosols in China*

Despite the recognized importance of aerosols for the simulation of climate in China, the quantification and understanding of their impacts are still poorly constrained. Difficulties arise especially on a regional scale, owing to the short atmospheric lifetime of the aerosol particles combined with the limited observations available. Simulated climate responses depend on simulated aerosol concentration, size, mixing state, AOD, activation of aerosol particles to form cloud droplets, as well as the cloud schemes in climate models. Current aerosol-climate models can simulate all these key parameters and processes, but nationwide long-term measurements are needed to constrain model simulations. The model uncertainties are especially large when aerosol-cloud interactions are included in simulations.

Since China is one of the most heavily polluted regions in the world, the impacts of air pollutants on hydrological cycle are of great concern. In recent decades, there has been a tendency of "southern flood and northern drought" over eastern China during the East Asian summer monsoon (Xu, 2001). Many modeling studies (e.g., Menon et al., 2002; Giorgi et al., 2002, 2003; Gu et al., 2006; Huang et al., 2007; Liu et al., 2009; Zhang et al., 2012b; Jiang et al., 2013; Wu et al., 2013) have shown that the East Asian summer monsoon precipitation is affected by aerosols, but contradictory results exist. Menon et al. (2002) suggested that the radiative effect of black carbon may contribute to a "southern flood and northern drought" pattern over eastern China. Liu et al. (2009) pointed out the aerosol radiative effect of sulfate is more dominant than that of black carbon in reducing precipitation over China. Gu et al. (2006) found that such a "southern flood and northern drought" pattern was due to the radiative effect of anthropogenic aerosols, which cooled the midlatitudes and led to the strengthening of the Hadley circulation. In contrast, Zhang et al. (2012b) showed that the aerosol direct radiative effect led to decreases in precipitation over southern China but slight increases in precipitation over northern China. Wu

et al. (2013) found that aerosol effects on precipitation depend on the location of monsoon precipitation band and its relative location to aerosols, which may be the main factor that contributed to the discrepancy in literature regarding the aerosol impacts on the so-called "southern flood and northern drought" over China.

Previous studies also reported the biases of using the fixed SSTs in the simulation of temperature and precipitation (Yue et al., 2011). The slow response associated with SST change caused by aerosols may play an important role in the simulated climate responses to aerosol forcing especially over ocean areas (Ganguly et al., 2012).
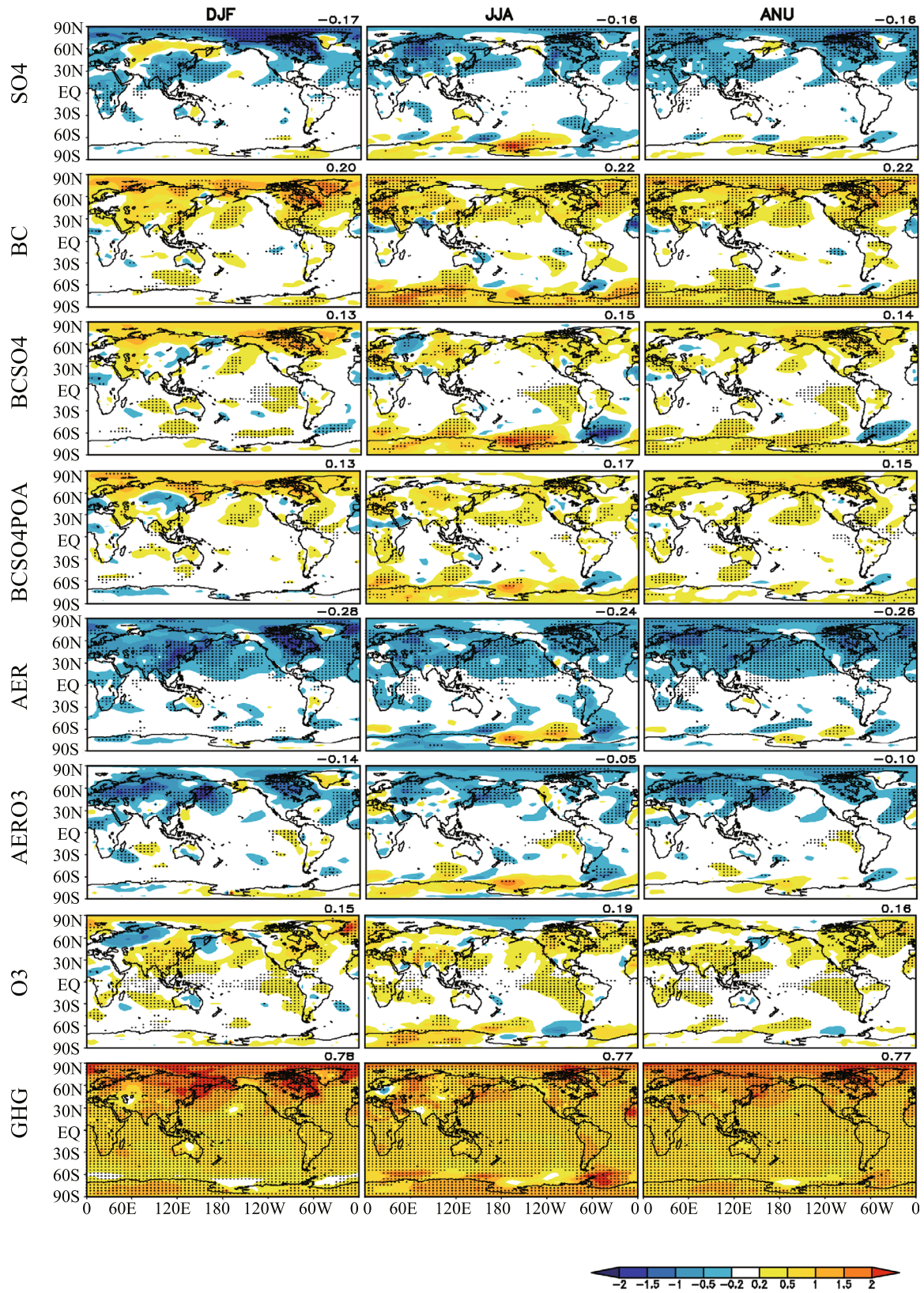
8. Summary and outlook

This review documents recent advances in our understanding of the climatic effects of O_3 and aerosols in China. All the key datasets or parameters needed for quantifying the effects of air pollutants on climate are reviewed, including emissions inventories, measurements of concentrations and column burdens, observed optical properties of aerosols, high correlations between air pollutants and the observed changes in meteorological parameters in China, estimated radiative forcing by O_3 and different aerosol species, as well as the simulated impacts of O_3 and aerosols on climate change in China.

During the past decade important advances have been made in our understanding of air pollutants and their roles in climate change in China. Emissions inventories of O_3/aerosol precursors and aerosols have become available for the Chinese domain, allowing concentrations of O_3 and different aerosol species to be simulated and their climatic effects estimated using numerical models. Increased ground and aircraft measurements of concentrations of O_3 and speciated aerosols in China, together with satellite measurements of aerosol optical properties and cloud properties, have provided datasets to constrain the simulated climatic effects of O_3 and aerosols. However, estimates of the climatic effects of air pollutants in China are still subject to large uncertainties. Based on this review, we suggest the following key priorities for future research:
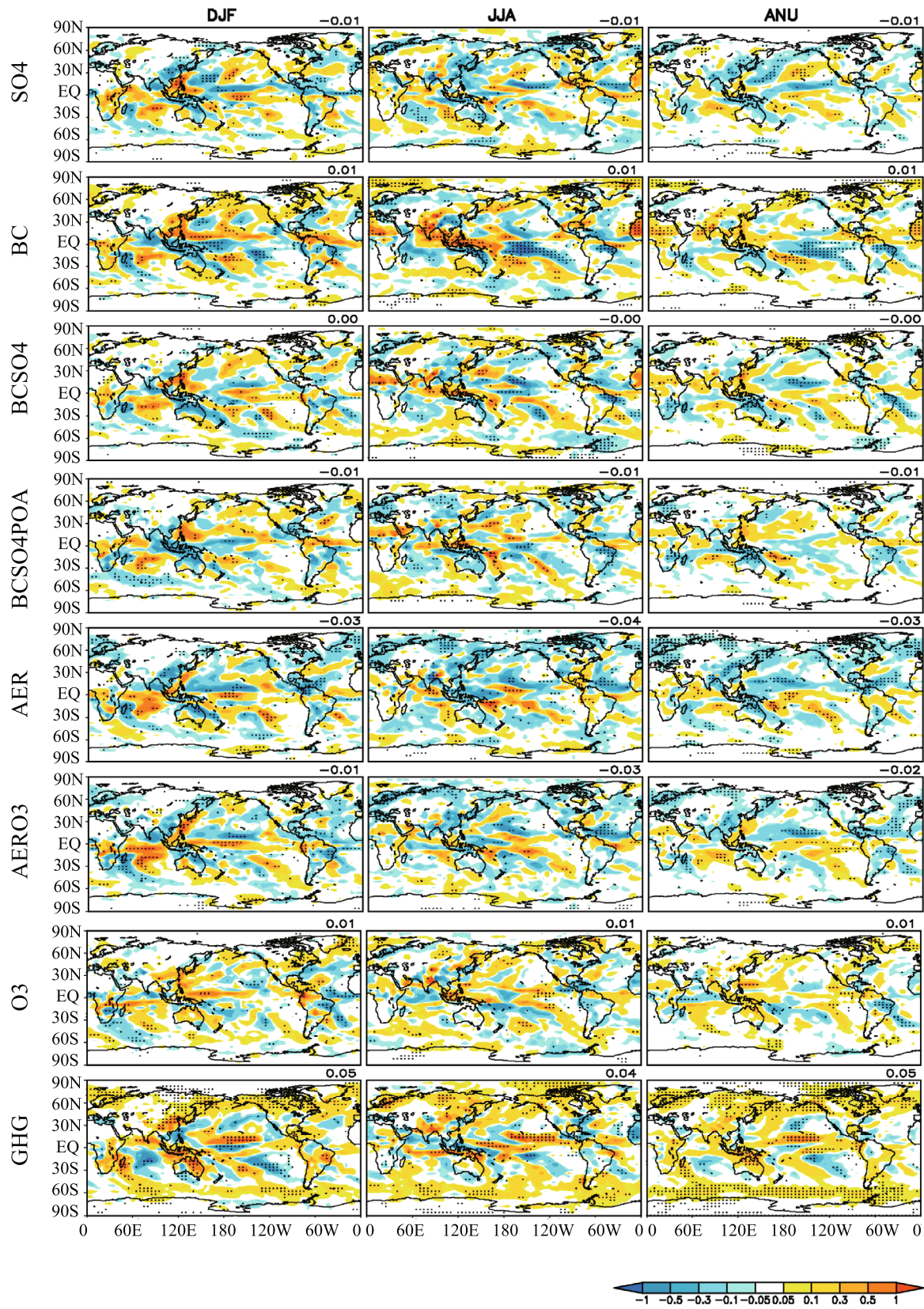
(1) Continued improvement in gas and particle emission inventories that underlie any predictions of climatological levels of pollutants. Since the emissions inventories from different research groups vary, it is necessary to quantify how the uncertainties in emissions can influence simulated climate change, such as changes in temperature and precipitation.

(2) Nationwide long-term measurements of concentrations and optical properties of pollutants. Measurements of speciated aerosol mass concentrations, size-resolved aerosol number concentrations, and aerosol–cloud interactions are important for reducing uncertainties associated with the climatic effect of aerosols. Special attention needs to be paid to the vertical profiles of concentrations and optical properties.

(3) Coupled transient chemistry–aerosol–climate simulations for interpreting climate change in China over past decades. While air pollutants can influence climate as sum-

Fig. 6. Predicted changes in December–January–February (DJF), June–July–August (JJA), and annual averaged surface air temperature (K) over the period 1950–2000 by different aerosol species, O$_3$, and GHGs. Dotted areas denote results that pass the t-test at the 95% confidence level. The global mean value is indicated in the top right corner of each panel. (Source: Chang et al., 2009).

Fig. 7. Predicted changes in December–January–February (DJF), June–July–August (JJA), and annual averaged precipitation (mm d^{-1}) over the period 1950–2000 by different aerosol species, O$_3$, and GHGs. Dotted areas denote results that pass the *t*-test at the 95% confidence level. The global mean value is indicated in the top right corner of each panel. (Source: Chang et al., 2009).

marized above, interannual and decadal variations in meteorological fields associated with Asian monsoon can influence air pollutants over China by influencing their transport, chemical reactions, and deposition (Zhu et al., 2012). Simulations also need to account for the role of SST responses to O_3/aerosol-induced forcing (Yue et al., 2011). Because of the monsoon system, changes in SST have large impacts on temperature gradient, atmospheric circulation, and water vapor supply from the oceans, resulting in complex feedbacks in regional climate. It should also be noted that tropospheric O_3 has been found to contribute to about 0.5 K of increases in surface air temperature in eastern China in past decades (Hansen et al., 2007; Chang et al., 2009); the radiative effect of tropospheric O_3 should be considered in simulations of climate change in China.

(4) Improved analysis of the aerosol indirect effect in China. As in other parts of the world, aerosol–cloud interaction is recognized as perhaps the most complex and uncertain issue in addressing anthropogenic impacts on climate change. The link between aerosol concentration and cloud optical properties depends on multiple factors (i.e., cloud droplet activation, updraft velocity etc.). The parameterizations of aerosol–cloud interactions in current climate models are generally not developed based on measurements in China, which need to be evaluated and improved to represent the chemical and meteorological conditions in this part of the world. More physical-based methods to determine cloud droplet concentrations from aerosol concentrations and other relevant parameters should be used in climate simulations. Furthermore, since precipitation during Asian summer monsoon is associated with strong convective clouds, the interactions between aerosols and strong convective clouds, as proposed by Rosenfeld et al. (2008), are expected to be important and should be the subject of future work.

REFERENCES

Ackerman, A. S., O. B. Toon, D. E. Stevens, A. J. Heymsfield, V. Ramanathan, and E. J. Welton, 2000: Reduction of tropical cloudiness by soot. *Science*, **288**, 1042–1047.

Albrecht, B. A., 1989: Aerosols, cloud microphysics, and fractional cloudiness. *Science*, **245**, 1227–1230.

Andreae, M. O., O. Schmid, H. Yang, D. Chand, J. Z. Yu, L. M. Zeng, and Y. H. Zhang, 2008: Optical properties and chemical composition of the atmospheric aerosol in urban Guangzhou, China. *Atmos. Environ.*, **42**, 6335–6350.

Bennartz, R., J. Fan, J. Rausch, L. R. Leung, and A. K. Heidinger, 2011: Pollution from China increases cloud droplet number, suppresses rain over the East China Sea. *Geophys. Res. Lett.*, **38**, L09704, doi: 10.1029/2011GL047235.

Bergin, M. H., and Coauthors, 2001: Aerosol radiative, physical,

and chemical properties in Beijing during June 1999. *J. Geophys. Res.*, **106**, 17 969–17 980.

Bo, Y., H. Cai, and S. D. Xie, 2008: Spatial and temporal variation of historical anthropogenic NMVOCs emission inventories in China. *Atmos. Chem. Phys.*, **8**, 7297–7316, doi: 10.5194/acp-8-7297-2008.

Bollasina, M. A., Y. Ming, and V. Ramaswamy, 2011: Anthropogenic aerosols and the weakening of the South Asian summer monsoon. *Science*, **334**(6055), 502–505, doi: 10.1126/science.1204994.

Boucher, O., and U. Lohmann, 1995: The sulfate-CCN-cloud albedo effect—A sensitivity study with two general circulation models. *Tellus B*, **47**, 281–300.

Carmichael, G. R., F. Martin, T. Narisara, and H. W. Jung, 2003: Measurements of sulfur dioxide, ozone and ammonia concentrations in Asia, Africa, and South America using passive samplers. *Atmos. Environ.*, **37**, 1293–1308.

Cao, J. J., S. C. Lee, K. F. Ho, X. Y. Zhang, S. C. Zou, K. Fung, J. C. Chow, and J. G. Watson, 2003: Characteristics of carbonaceous aerosol in Pearl River Delta Region, China during 2001 winter period. *Atmos. Environ.*, **37**(11), 1451–1460.

Cao, J. J., S. C. Lee, and K. F. Ho, 2004: Spatial and seasonal variations of atmospheric organic carbon and elemental carbon in Pearl River Delta Region, China. *Atmos. Environ*, **38**(27), 4447–4456.

Cao, J. J., and Coauthors, 2007: Spatial and seasonal distributions of carbonaceous aerosols over China. *J. Geophys. Res.*, **112**, D22S11, doi: 10.1029/2006JD008205.

Cao, J. J., Z. X. Shen, J. C. Chow, G. W. Qi, and J. C. Watson, 2009: Seasonal variations and sources of mass and chemical composition for PM(10) aerosol in Hangzhou, China. *Particuology*, **7**(3), 161–168.

Cao, L., P. Zhao, Z. Yan, P. Jones, Y. Zhu, Y. Yu, and G. Tang, 2013: Instrumental temperature series in eastern and central China back to the nineteenth century. *J. Geophys. Res.*, **118**, doi: 10.1002/jgrd.50615.

Chan, C. Y., L. Y. Chan, W. L. Chang, Y. G. Zheng, H. Cui, X. D. Zheng, Y. Qin, and Y. S. Li, 2003: Characteristics of a tropospheric ozone profile and implications for the origin of ozone over subtropical China in the spring of 2001. *J. Geophys. Res.*, **108** (D20), 8800, doi: 10.1029/2003JD003427.

Chang, W. Y., and H. Liao, 2009: Anthropogenic direct radiative forcing of tropospheric ozone and aerosols from 1850 to 2000 estimated with IPCC AR5 emissions inventories. *Atmos. Oceanic Sci. Lett.*, **2**, 201–207.

Chang, W. Y., H. Liao, and H. Wang, 2009: Climate responses to direct radiative forcing of anthropogenic aerosols, tropospheric ozone, and long-lived greenhouse gases in eastern China over 1951–2000. *Adv. Atmos. Sci.*, **26**, 748–762, doi: 10.1007/s00376-009-9032-4.

Che, H. Z., G. Y. Shi, X. Y. Zhang, R. Arimoto, J. Q. Zhao, L. Xu, B. Wang, and Z. H. Chen, 2005: Analysis of 40 years of solar radiation data from China, 1961–2000. *Geophys. Res. Lett.*, **32**, L06803, doi: 10.1029/2004GL022322.

Che, H. Z., X. Y. Zhang, Y. Li, Z. Zhou, and J. J. Qu, 2007: Horizontal visibility trends in China 1981–2005. *Geophys. Res. Lett.*, **34**, L24706, doi: 10.1029/2007GL031450.

Chen, L.-X., B. Zhang, W.-Q. Zhu, X.-J. Zhou, Y.-F. Luo, Z.-J. Zhou, and J.-H. He, 2009: Variation of atmospheric aerosol optical depth and its relationship with climate change in China east of 100°E over the last 50 years. *Theor. Appl. Climatol.*, **96**, 191–199.

Chen, W.-T., H. Liao, and J. H. Seinfeld, 2007: Future climate impacts of direct radiative forcing of anthropogenic aerosols, tropospheric ozone, and long-lived greenhouse gases. *J. Geophys. Res.*, **112**, D14209, doi: 10.1029/2006JD008051.

Cheng, Y., U. Lohmann, J. Zhang, Y. Luo, Z. Liu, and G. Lesins, 2005: Contribution of changes in sea surface temperature and aerosol loading to the decreasing precipitation trend in southern China. *J. Climate*, **18**, 1381–1390.

Cheng, Y. F., and Coauthors, 2008: Aerosol optical properties and related chemical apportionment at Xinken in Pearl River Delta of China. *Atmos. Environ.*, **42**, 6351–6372.

Choi, Y.-S., C.-H. Ho, J. Kim, D.-Y. Gong, and R. J. Park, 2008: The impact of aerosols on the summer rainfall frequency in China. *J. Appl. Meteor. Climate*, **47**, 1802–1813.

Dan, M., G. S. Zhuang, X. X. Li, H. R. Tao, and Y. H. Zhuang, 2004: The characteristics of carbonaceous species and their sources in PM2.5 in Beijing. *Atmos. Environ.*, **38**(21), 3443–3452.

Deng, X. J., X. X. Tie, D. Wu, X. J. Zhou, X. Y. Bi, H. B. Tan , F. Li, and C. L. Jiang, 2008: Long-term trend of visibility and its characterizations in the Pearl River Delta (PRD) region, China. *Atmos. Environ.*, **42**(7), 1424–1435.

Ding, A. J., T. Wang, V. Thouret, J. P. Cammas, and P. Nédélec, 2008: Tropospheric ozone climatology over Beijing: Analysis of aircraft data from the MOZAIC program. *Atmos. Chem. Phys.*, **8**, 1–13.

Du, W. P., J. Y. Xin, M. X. Wang, Q. X. Gao, Z. Q. Li, and Y. S. Wang, 2008: Photometric measurements of spring aerosol optical properties in dust and non-dust periods in China. *Atmos. Environ.*, **42**(34), 7981–7987.

Duan, F. K., X. D. Liu, T. Yu, and H. Cachier, 2004: Identification and estimate of biomass burning contribution to the urban aerosol organic carbon concentrations in Beijing. *Atmos. Environ.*, **38**(9), 1275–1282.

Duan, F. K., K. He, Y. L. Ma, F. M. Yang, X. C. Yu, S. H. Cadle, T. Chan, and P. A. Mulawa, 2006: Concentration and chemical characteristics of PM2.5 in Beijing, China: 2001–2002. *Sci. Total Environ.*, **355**, 264–275.

Duan, J., and J. T. Mao, 2009: Influence of aerosol on regional precipitation in North China. *Chinese Science Bulletin*, **54**(3), 474–483.

Dufour, G., M. Eremenko, J. Orphal, and J.-M. Flaud, 2010: IASI observations of seasonal and day-to-day variations of tropospheric ozone over three highly populated areas of China: Beijing, Shanghai, and Hong Kong. *Atmos. Chem. Phys.*, **10**, 3787–3801, doi: 10.5194/acp-10-3787-2010.

Fan, X. H., H. B. Chen, X. G. Xia, Z. Q. Li, and M. Cribb, 2010: Aerosol optical properties from the atmospheric radiation measurement mobile facility at Shouxian, China. *J. Geophys. Res.*, **115**, D00K33, doi: 10.1029/2010JD014650.

Feng, Y. L., Y. J. Chen, H. Gao, G. R. Zhi, S. C. Xiong, J. Li, G. Y. Sheng, and J. M. Fu, 2009: Characteristics of organic and elemental carbon in PM2.5 samples in Shanghai, China. *Atmos. Res.*, **92**(4), 434–442.

Fu, Y., and H. Liao, 2012: Simulation of the interannual variations of biogenic emissions of volatile organic compounds in China: Impacts on tropospheric ozone and secondary organic aerosol. *Atmos. Environ.*, **59**, 170–785.

Ganguly, D., P. J. Rasch, H. Wang, J.-H. Yoon, 2012: Fast and slow responses of the South Asian monsoon system to anthropogenic aerosols. *Geophys. Res. Lett.*, **39**, L18804, Doi: 10.1029/2012GL053043.

Gao, H. W., J. Chen, B. Wang, S. C. Tan, C. M. Lee, X. H. Yao, H. Yan, and J. H. Shi, 2011: A study of air pollution of city clusters. *Atmos. Environ.*, **45**(18), 3069–3077.

Garland, R. M., and Coauthors, 2009: Aerosol optical properties observed during Campaign of Air Quality Research in Beijing 2006 (CAREBeijing-2006): Characteristic differences between the inflow and outflow of Beijing city air. *J. Geophys. Res.*, **114**, D00G04, doi: 10.1029/2008JD010780.

Ghan, S. J., L. R. Leung, R. C. Easter, and H. Abdul-Razzak, 1997: Prediction of cloud droplet number in a general circulation model. *J. Geophys. Res.*, **102**(D18), 21 777–21 794, doi: 10.1029/97JD01810.

Giorgi, F., X. Bi, and Y. Qian, 2002: Direct radiative forcing and regional climatic effects of anthropogenic aerosols over East Asia: A regional coupled climate-chemistry/aerosol model study. *J. Geophys. Res.*, **107**(D20), 4439, doi: 10.1029/2001 JD001066.

Giorgi, F., X. Q. Bi, and Y. Qian, 2003: Indirect vs. direct effects of anthropogenic sulfate on the climate of East Asia as simulated with a regional coupled climate-chemistry/aerosol model. *Climatic Change*, **58**(3), 345–376.

Gu, Y., K. N. Liou, Y. Xue, C. R. Mechoso, W. Li, and Y. Luo, 2006: Climatic effects of different aerosol types in China simulated by the UCLA general circulation model. *J. Geophys. Res.*, **111**, D15201, doi: 10.1029/2005JD006312.

Han, Z., 2010: Direct radiative effect of aerosols over East Asia with a regional coupled climate/chemistry model. *Meteorologische Zeitschrift*, **19**(3), 287–298.

Hansen, J., M. Sato, and R. Ruedy, 1997: Radiative forcing and climate response. *J. Geophys. Res.*, **102**, 6831–6864.

Hansen, J., and Coauthors, 2007: Climate simulations for 1880–2003 with GISS modelE. *Climate Dyn.*, **29**(7–8), 661–696.

He, K., and Coauthors, 2001: The characteristics of PM2.5 in Beijing, China. *Atmos. Environ.*, **35**, 4 959–4 970.

He, X., C. C. Li, A. K. Lau, Z. Z. Deng, J. T. Mao, M. H. Wang, and X. Y. Liu, 2009: An intensive study of aerosol optical properties in Beijing urban area. *Atmos. Chem. Phys.*, **9**, 8903–8915.

Huang, Y., R. E. Dickinson, and W. L. Chameides, 2006: Impact of aerosol indirect effect on surface temperature over East Asia. *Proc. Natl. Acad. Sci. USA*, **103**(12), 4371–4376.

Huang, Y., W. L. Chameides, and R. E. Dickinson, 2007: Direct and indirect effects of anthropogenic aerosols on regional precipitation over East Asia. *J. Geophys. Res.*, **112**, D03212, doi: 10.1029/2006JD007114.

Ho, K. F., J. J. Cao, S. C. Lee, and C. K. Chan, 2006: Source apportionment of PM2.5 in urban area of Hong Kong. *Journal of Hazardous Materials*, **138**(1), 73–85.

Hou, B., G. Zhuang, R. Zhang, T. Liu, Z. Guo, and Y. Chen, 2011: The implication of carbonaceous aerosol to the formation of haze: Revealed from the characteristics and sources of OC/EC over a mega-city in China. *Journal of Hazardous Materials*, **190**(1–3), 529–536.

IPCC, 1995: *Climate Change 1995: The Science of Climate Change. Contribution of Working Group I to the Second Assessment Report of the Intergovernmental Panel on Climate Change*, Cambridge University Press, Cambridge, United Kingdom and New York, NY, USA, 584 pp.

IPCC, 2007: *Climate Change 2007: The Physical Science Basis. Contribution of Working Group I to the Fourth Assessment Report of the Intergovernmental Panel on Climate Change*, Cambridge University Press, Cambridge, United Kingdom and New York, NY, USA, 996 pp.

IPCC, 2013: *Climate Change 2013: The Physical Science Basis. Contribution of Working Group I to the Fifth Assessment Report of the Intergovernmental Panel on Climate Change*, Cambridge University Press, Cambridge, United Kingdom and New York, NY, USA, 1535 pp.

Ianniello, A., F. Spataro, G. Esposito, I. Allegrini, M. Hu, and T. Zhu, 2011: Chemical characteristics of inorganic ammonium salts in PM2.5 in the atmosphere of Beijing (China). *Atmos. Chem. Phys.*, **11**, 10 803–10 822, doi: 10.5194/acp-11-10803-2011.

Jiang, Y., X. Liu, X.-Q. Yang, and M. Wang, 2013: A numerical study of the effect of different aerosol types on East Asian summer clouds and precipitation. *Atmos. Environ.*, **70**, 51–63.

Kaiser, D. P., and Y. Qian, 2002: Decreasing trends in sunshine duration over China for 1954–1998: Indication of increased haze pollution? *Geophys. Res. Lett.*, **29**(21), 38-1–38-4, doi: 10.1029/2002GL016057.

Kim, D.-H., B.-J. Sohn, T. Nakajima, T. Takamura, T. Takemura, B.C. Choi, and C. Yoon, 2004: Aerosol optical properties over East Asia determined from ground-based sky radiation measurements. *J. Geophys. Res.*, **109**, D02209, doi: 10.1029/2003JD003387.

Kim, M.-K., W. K. M. Lau, K.-M. Kim, and W.-S. Lee, 2007: A GCM study of effects of radiative forcing of sulfate aerosol on large scale circulation and rainfall in East Asia during boreal spring. *Geophys. Res. Lett.*, **34**, L24701, doi: 10.1029/2007GL031683.

Lau, K. M., and K. M. Kim, 2006: Observational relationships between aerosol and Asian monsoon rainfall, and circulation. *Geophys. Res. Lett.*, **33**, L21810, doi: 10.1029/2006GL027546.

Lee, K. H., Z. Q. Li, M. S. Wong, J. Y. Xin, Y. S. Wang, W. M, Hao, and F. S. Zhao, 2007: Aerosol single scattering albedo estimated across China from a combination of ground and satellite measurements. *J. Geophys. Res.*, **112**, D22S15, doi: 10.1029/2007JD009077.

Lei, Y., Q. Zhang, K. B. He, and D. G. Streets, 2011: Primary anthropogenic aerosol emission trends for China, 1990–2005. *Atmos. Chem. Phys.*, **11**, 931–954, doi: 10.5194/acp-11-931-2011.

Li, C., and Coauthors, 2007a: In situ measurements of trace gases and aerosol optical properties at a rural site in northern China during East Asian Study of Tropospheric Aerosols: An International Regional Experiment 2005. *J. Geophys. Res.*, **112**, D22S04, doi: 10.1029/2006JD007592.

Li, J., W.-C. Wang, H. Liao, and W. Chang, 2014: Past and future direct radiative forcing of nitrate aerosol in East Asia. *Theor. Appl. Climatol.*, in press.

Li, J. P., and Q. C. Zeng, 2002: A unified monsoon index. *Geophys. Res. Lett.*, **29**(8), 115-1–115-4, doi: 10.1029/2001GL013874.

Li, J. P., and Q. C. Zeng, 2003: A new monsoon index and the geographical distribution of the global monsoons. *Adv. Atmos. Sci.*, **20**, 299–302, doi: 10.1007/s00376-003-0016-5.

Li, J. P., and Q. C. Zeng, 2005: A new monsoon index, its interannual variability and relation with monsoon precipitation. *Climatic and Environmental Research*, **10**, 351–365. (in Chinese)

Li, L. J., B. Wang, and T. J. Zhou, 2007b: Contributions of natural and anthropogenic forcings to the summer cooling over eastern China: An AGCM study. *Geophys. Res. Lett.*, **34**, L18807, doi: 10.1029/2007GL030541.

Li, W. G., M. T. Hou, and J. W. Xin, 2011a: Low-cloud and sun-

shine duration in the low-latitude belt of South China for the period 1961–2005. *Theor. Appl. Climatol.*, **104**, 473–478, doi: 10.1007/s00704-010-0360-1.

Li, X. S., Z. S. He, X. M. Fang, and X. J. Zhou, 1999: Distribution of surface ozone concentration in the clean areas of China and its possible impact on crop yields. *Adv. Atmos. Sci.*, **16**, 154–158.

Li, Z., and Z.-W. Yan, 2009: Homogenized daily mean/maximum/minimum temperature series for China from 1960–2008. *Atmos. Oceanic Sci. Lett.*, **2**, 237–243.

Li, Z., and Coauthors, 2007c: Preface to special section on East Asian Studies of Tropospheric Aerosols: An International Regional Experiment (EAST-AIRE). *J. Geophys. Res.*, **112**, D22S00, doi: 10.1029/2007JD008853.

Li, Z., and Coauthors, 2011b: East Asian Studies of Tropospheric Aerosols and their Impact on Regional Climate (EAST-AIRC): An overview. *J. Geophys. Res.*, **116**, D00K34, doi: 10.1029/2010JD015257.

Liang, F., and X. A. Xia, 2005: Long-term trends in solar radiation and the associated climatic factors over China for 1961–2000. *Annales Geophysicae*, **23**, 2425–2432.

Lin, W., X. Xu, X. Zhang, and J. Tang, 2008: Contributions of pollutants from North China Plain to surface ozone at the Shangdianzi GAW Station. *Atmos. Chem. Phys.*, **8**, 5889–5898, doi: 10.5194/acp-8-5889-2008.

Liu, J., Y. Zheng, Z. Li, and R. Wu, 2008: Ground-based remote sensing of aerosol optical properties in one city in Northwest China. *Atmos. Res.*, **89**, 194–205.

Liu, X., and Coauthors, 2006: First directly retrieved global distribution of tropospheric column ozone from GOME: Comparison with the GEOS-CHEM model. *J. Geophys. Res.*, **111**, D02308, doi: 10.1029/2005JD006564.

Liu, Y., J. Sun, and B. Yang, 2009: The effects of black carbon and sulfate aerosols in China regions on East Asia monsoons. *Tellus*, **61B**, 642–656, doi: 10.1111/j.1600-0889.2009.00427.x.

Lyapustin, A., and Coauthors, 2011: Reduction of aerosol absorption in Beijing since 2007 from MODIS and AERONET. *Geophys. Res. Lett.*, **38**, L10803, doi: 10.1029/2011GL047306.

Ma, N., and Coauthors, 2011: Aerosol optical properties in the North China Plain during HaChi campaign: an in-situ optical closure study. *Atmos. Chem. Phys.*, **11**, 5959–5973.

Meng, Z. Y., X. B. Xu, P. Yan, G. A. Ding, J. Tang, W. L. Lin, X. D. Xu, and S. F. Wang, 2009: Characteristics of trace gaseous pollutants at a regional background station in Northern China. *Atmos. Chem. Phys.*, **8**, 927–936, doi: 10.5194/acp-9-927-2009.

Menon, S., J. Hansen, L. Nazarenko, and Y. Luo, 2002: Climate effects of black carbon aerosols in China and India. *Science*, **297**, 2250–2253.

Muller, D., and Coauthors, 2006: Strong particle light absorption over the Pearl River Delta (south China) and Beijing (north China) determined from combined Raman lidar and Sun photometer observations. *Geophys. Res. Lett.*, **33**, L20811, doi: 10.1029/2006GL027196.

Qian, Y., L. R. Leung, S. J. Ghan, and F. Giorgi, 2003: Regional climate effects of aerosols over China: modeling and observation. *Tellus*, **55B**, 914–934.

Qian, Y., W. Wang, L. R. Leung, and D. P. Kaiser, 2007: Variability of solar radiation under cloud-free skies in China: The role of aerosols. *Geophys. Res. Lett.*, **34**, L12804, doi: 10.1029/2006GL028800.

Qian, Y., D. Y. Gong, J. W. Fan, L. R. Leung, R. Bennartz, D.

L. Chen, and W. G. Wang, 2009: Heavy pollution suppresses light rain in China: Observations and modeling. *J. Geophys. Res.*, **114**, D00K02, doi: 10.1029/2008JD011575.

Qiu, J., and J. Yang, 2008: Absorption properties of urban/suburban aerosols in China. *Adv. Atmos. Sci.*, **25**, 1–10, doi: 10.1007/s00376-008-0001-0.

Qiu, J. H., L. Q. Yang, and X. Y. Zhang, 2004: Characteristics of the imaginary part and single-scattering albedo of urban aerosols in northern China. *Tellus*, **56B**, 276–284.

Ramanathan, V., P. J. Crutzen, J. T. Kiehl, and D. Rosenfeld, 2001: Aerosols, Climate and the Hydrological cycle. *Science*, **294**, 2119–2124, doi: 10.1126/science.1064034.

Ramanathan, V., and Coauthors, 2005: Atmospheric brown clouds: Impacts on South Asian climate and hydrological cycle. *Proc. Natl. Acad. Sci. USA*, **102**, 326–5333.

Rosenfeld, D., U. Lohmann, G. B. Raga, C. D. O'Dowd, M. Kulmala, S. Fuzzi, A. Reissell, and M. O. Andreae, 2008: Flood or drought: How do aerosols affect precipitation? *Science*, **321**, 1309–1313, doi: 10.1126/science.1160606.

Shi, X. H., X. D. Xu, and L. Xie, 2008: Characteristics of climate change in the "Significant Impact Zone" affected by aerosols over eastern China in warm seasons. *Sci. China* (D), **51**(5), 730–39.

Sun, Y. L., G. S. Zhuang, and W. Ying, 2004: The air-borne particulate pollution in Beijing—concentration, composition, distribution and sources. *Atmos. Environ.*, **38**(35), 5991–6004.

Sun, Y. L., Z. F. Wang, H. B. Dong, T. Yang, J. Li, X. L. Pan, P. Chen, and J. T. Jayne, 2012: Characterization of summer organic and inorganic aerosols in Beijing, China with an aerosol chemical speciation monitor. *Atmos. Environ.*, **51**, 250–259.

Streets, D. G., and K. Aunan, 2005: The importance of China's household sector for black carbon emissions. *Geophys. Res. Lett.*, **32**, L12708, doi: 10.1029/2005GL022960.

Streets, D. G., and Coauthors, 2003: An inventory of gaseous and primary aerosol emissions in Asia in the year 2000. *J. Geophys. Res.*, **108** (D21), 8809, doi: 10.1029/2002JD003093.

Tang, G., X. Li, Y. Wang, J. Xin, and X. Ren, 2009: Surface ozone trend details and interpretations in Beijing, 2001–2006. *Atmos. Chem. Phys.*, **9**, 8813–8823, doi: 10.5194/acp-9-8813-2009.

Tang J., P. Wang, L. J. Mickley, X. Xia, H. Liao, X. Yue, L. Sun, and J. Xia, 2014: Positive relationship between liquid cloud droplet effective radius and aerosol optical depth over Eastern China from satellite data. *Atmos. Environ.*, **84**, 244–253, doi: 10.1016/j.atmosenv.2013.08.024, 2014.

Takami, A., W. Wang, D. G. Tang, and S. Hatakeyama, 2006: Measurements of gas and aerosol for two weeks in northern China during the winter-spring period of 2000, 2001 and 2002. *Atmos. Res.*, **82**(3–4), 688–697.

Takemura, T., T. Nozawa, S. Emori, T. Y. Nakajima, and T. Nakajima, 2005: Simulation of climate response to aerosol direct and indirect effects with aerosol transport-radiation model. *J. Geophys. Res.*, **110**, D02202, doi: 10.1029/2004JD005029.

Tao, J., T. T. Cheng, R. J. Zhang, J. J. Cao, L. H. Zhu, Q. Y. Wang, L. Luo, and L. M. Zhang, 2013: Chemical composition of PM2.5 at an urban site of Chengdu in southwestern China. *Adv. Atmos. Sci.*, **30**(4), 1070–1084, doi: 10.1007/s00376-012-2168-7.

Tu, J., Z.-G. Xia, H. S. Wang, and W. Q. Li, 2007: Temporal variations in surface ozone and its precursors and meteorological effects at an urban site in China. *Atmos. Res.*, **85**(3–4), 310–337.

Twomey, S., 1959: The nuclei of natural cloud formation. II. The supersaturation in natural clouds and the variation of cloud droplet concentration. *Geofisica Pura e Applicata*, **43**, 243–249.

Twomey, S. A., 1977: The influence of pollution on the shortwave albedo of clouds. *J. Atmos. Sci.*, **34**, 1149–1152.

Wang, B., Z. Wu, J.-P. Li, J. Liu, C.-P. Chang, Y. Ding, and G.-X. Wu, 2008: How to Measure the Strength of the East Asian Summer Monsoon? *J. Climate*, **21**, 4449–4463. doi: 10.1175/2008JCLI2183.1.

Wang, G. H., L. M. Huang, S. X. Gao, S. T. Gao, and L. S. Wang, 2002: Characterization of water-soluble species of PM10 and PM2.5 aerosols in urban area in Nanjing, China. *Atmos. Environ.*, **36**(8), 1299–1307.

Wang, K. C., R. E. Dickinson, and S. L. Liang, 2009: Clear sky visibility has decreased over land globally from 1973 to 2007. *Science*, **323**, 1468–1470, doi: 10.1126/science.1167549.

Wang, S., J. Zhu, and J. Cai, 2004a: Interdecadal variability of temperature and precipitation in China since 1880. *Adv. Atmos. Sci.*, **21**(3), 307–313, doi: 10.1007/BF02915560.

Wang, T., H. L. A. Wong, J. Tang, A. Ding, W. S. Wu, and X. C. Zhang, 2006a: On the origin of surface ozone and reactive nitrogen observed at a remote mountain site in the northeastern Qinghai-Tibetan Plateau, western China. *J. Geophys. Res.*, **111**, D08303, doi: 10.1029/2005JD006527.

Wang, T. J., M. Xie, L. J. Gao, and H. M. Yang, 2004b: Development and preliminary application of a coupled regional climate-chemistry model system. *Journal of Nanjing University* (*Natural Sciences*), **40**(6), 711–727. (in Chinese)

Wang, T., S. Li, Y. Shen, J. Deng, and M. Xie, 2010: Investigations on direct and indirect effect of nitrate on temperature and precipitation in China using a regional climate chemistry modeling system. *J. Geophys. Res.*, **115**, D00K26, doi: 10.1029/2009JD013264.

Wang, W. G., J. Wu, and H. N. Liu, S. C. Guo, X. M. Chen, and Y. Luo, 2005a: Researches on the influence of pollution emission on tropospheric ozone variation and radiation over China and its adjacent area, Chinese. *J. Atmos. Sci.*, **29**(5), 734–746. (in Chinese)

Wang, Y., G. S. Zhuang, A. Tang, H. Yuan, Y. Sun, S. Chen, and A. H. Zheng, 2005b: The ion chemistry and the source of PM2.5 aerosol in Beijing. *Atmos. Environ.*, **39**(21), 3771–3784.

Wang, Y., G. S. Zhuang, X. Y. Zhang, K. Huang, C. Xu, A. Tang, J. M. Chen, and Z. S. An, 2006b: The ion chemistry, seasonal cycle, and sources of PM2.5 and TSP aerosol in Shanghai. *Atmos. Environ.*, **40**(16), 2935–2952.

Wang, Y., Y. Zhang, J. Hao, and M. Luo, 2011: Seasonal and spatial variability of surface ozone over China: Contributions from background and domestic pollution. *Atmos. Chem. Phys.*, **11**, 3511–25.

Wang, Y., B. Hu, G. Tang, D. Ji, H. Zhang, J. Bai, X. Wang, and Y. Wang, 2013: Characteristics of ozone and its precursors in Northern China: A comparative study of three sites. *Atmospheric Research*, **132**: 450–459, doi: 10.1016/j.atmosres.2013.04.005.

Wendisch, M., and Coauthors, 2008: Radiative and dynamic effects of absorbing aerosol particles over the Pearl River Delta, China. *Atmos. Environ.*, **42**, 6405–6416.

Wu, J., W. Jiang, C. Fu, B. Su, H. Liu, and J. Tang, 2004: Simulation of the radiative effect of black carbon aerosols and the regional climate response over China. *Adv. Atmos. Sci.*, **21**(4), 637–649, doi: 10.1007/BF02915731.

Wu, J., C. Fu, Y. Xu, J. P. Tang, W. Wang, and Z. Wang, 2008: Simulation of direct effects of black carbon aerosol on temperature and doi: Hydrological cycle in Asia by a Regional Climate Model. *Meteor. Atmos. Phys.*, **100**, 179–193, doi: 10.1007/s00703-008-0302-y.

Wu, L., H. Su, and J. H. Jiang, 2013: Regional simulation of aerosol impacts on precipitation during the East Asian summer monsoon. *J. Geophys. Res.*, **118**, 6454–6467, doi: 10.1002/jgrd.50527.

Wu, W. S., and T. Wang, 2007: On the performance of a semi-continuous PM2.5 sulphate and nitrate instrument under high loadings of particulate and sulphur dioxide. *Atmos. Environ.*, **41**, 5442–5451.

Xia, X.-A., H.-B. Chen, P.-C. Wang, X. M. Zong, J. H. Qiu, and G. Philippe, 2005: Aerosol properties and their spatial and temporal variations over North China in spring 2001. *Tellus*, **57B**, 28–39.

Xia, X. A., H. B. Chen, P. C. Wang, W. X. Zhang, P. Goloub, B. Chatenet, T. F. Eck, and B. N. Holben, 2006: Variation of column-integrated aerosol properties in a Chinese urban region. *J. Geophys. Res.*, **111**, D05204, doi: 10.1029/2005JD006203.

Xia, X. A., H. Chen, P. Goloub, W. Zhang, B. Chatenet, and P. Wang, 2007a: A compilation of aerosol optical properties and calculation of direct radiative forcing over an urban region in northern China. *J. Geophys. Res.*, **112**, D12203, doi: 10.1029/2006JD008119.

Xia, X. A., Z. Q. Li, B. Holben, P. Wang, T. Eck, H. B. Chen, M. Cribb, and Y. X. Zhao, 2007b: Aerosol optical properties and radiative effects in the Yangtze Delta region of China. *J. Geophys. Res.*, **112**, D22S12, doi: 10.1029/2007JD008859.

Xu, J., M. H. Bergin, X. Yu, G. Liu, J. Zhao, C. M. Carrico, and K. Baumann, 2002: Measurement of aerosol chemical, physical and radiative properties in the Yangtze delta region of China. *Atmos. Environ.*, **36**, 161–173.

Xu, J., M. H. Bergin, R. Greenwald, J. J. Schauer, M. M. Shafer, J. L. Jaffrezo, and G. Aymoz, 2004: Aerosol chemical, physical, and radiative characteristics near a desert source region of northwest China during ACE-Asia. *J. Geophys. Res.*, **109**, D19S03, doi: 10.1029/2003JD004239.

Xu, J., and Coauthors, 2007: Componental characteristics and sources identification of PM2.5 in Beijing. *J. Appl. Meteor. Sci.*, **18**, 646–654.

Xu, J., C. Li, H. Shi, Q. He, and L. Pan, 2011: Analysis on the impact of aerosol optical depth on surface solar radiation in the Shanghai megacity, China. *Atmos. Chem. Phys.*, **11**, 3281–3289, doi: 10.5194/acp-11-3281-2011.

Xin, J. Y., Y. S. Wang, Z. Q. Li, P. C. Wang, S. G. Wang, T. X. Wen, and Y. Sun, 2006: Introduction and calibration of the Chinese Sun hazemeter network. *Chinese Journal of Environmental Science*, **27**(9), 1697–1702. (in Chinese)

Xin, J. Y., and Coauthors, 2007: Aerosol optical depth (AOD) and angstrom exponent of aerosols observed by the Chinese Sun Hazemeter Network from August 2004 to September 2005. *J. Geophys. Res.*, **112**, D05203, doi: 10.1029/2006JD007075.

Xu, L. L., X. Q. Chen, J. S. Chen, F. W. Zhang, C. He, J. P. Zhao, and L. Q. Yin, 2012: Seasonal variations and chemical compositions of PM2.5 aerosol in the urban area of Fuzhou, China. *Atmospheric Research*, **104**, 264–272.

Xu, Q., 2001: Abrupt change of the mid-summer climate in central East China by the influence of atmospheric pollution. *Atmos. Environ.*, **35**(30), 5029–5040.

Xu, X., W. Lin, T. Wang, P. Yan, J. Tang, Z. Meng, and Y. Wang, 2008: Long-term trend of surface ozone at a regional background station in eastern China 1991–2006: Enhanced variability. *Atmos. Chem. Phys.*, **8**, 2595–2607.

Yan, L., X. Liu, P. Yang, Z.-Y. Yin, and G. R. North, 2011: Study of the impact of summer monsoon circulation on spatial distribution of aerosol in East Asia based on numerical simulations. *J. Appl. Meteor.*, **50**(11), 2270–2282, doi: 10.1175/2011JAMC-D-11-06.1.

Yan, P., and Coauthors, 1997: Observational Analysis of Surface O_3、NO_x, and SO_2 in China. *Applied Meteorology*, **8**(1), 53–61. (in Chinese)

Yan, P., M. L. Wang, H. B. Cheng, and X. J. Zhou, 2003: Distributions and variations of surface ozone in Changshu, Yangtze Delta region. *Acta Metallurgica Sinica*, **17**, 205–217. (in Chinese)

Yan, P., and Coauthors, 2008: The measurement of aerosol optical properties at a rural site in Northern China. *Atmos. Chem. Phys.*, **8**, 2229–2242.

Yang, F., and Coauthors, 2011: Characteristics of PM2.5 speciation in representative megacities and across China. *Atmos. Chem. Phys.*, **11**(1), 5207–5219.

Yang, H., J. Z. Yu, and S. S. H. Ho, 2005: The chemical composition of inorganic and carbonaceous materials in PM2.5 in Nanjing, China. *Atmos. Environ.*, **39**(20), 3735–3749.

Ye, B., X. Ji, H. Yang, X. Yao, C. K. Chan, S. H. Cadle, T. Chan, and P. A. Mulawa, 2003: Concentration and chemical composition of PM2.5 in shanghai for a 1-year period. *Atmos. Environ.*, **37**, 499–510.

Yu, X., B. Zhu, and M. Zhang, 2009: Seasonal variability of aerosol optical properties over Beijing. *Atmos. Environ.*, **43**, 4095–4101.

Yue, X., H. Liao, H. J. Wang, S. L. Li, and J. P. Tang, 2011: Role of sea surface temperature responses in simulation of the climatic effect of mineral dust aerosol. *Atmos. Chem. Phys.*, **11**, 6049–6062, doi: 10.5194/acp-11-6049-2011.

Zhang, F., H.-R. Cheng, Z.-W. Wang, X.-P. Lv, Z.-M. Zhu, G. Zhang, and X.-M. Wang, 2014: Fine particles (PM2.5) at a CAWNET background site in Central China: Chemical compositions, seasonal variations and regional pollution events. *Atmos. Environ.*, **86**, 193–202, doi: 10.1016/j.atmosenv.2013.12.008.

Zhang, L., H. Liao, and J. P. Li, 2010: Impacts of Asian summer monsoon on seasonal and interannual variations of aerosols over eastern China. *J. Geophys. Res.*, **115**, D00K05, doi: 10.1029/2009JD012299.

Zhang, Q., J. N. Quan, X. X. Tie, M. Y. Huang, and X. C. Ma, 2011: Impact of aerosol particles on cloud formation: Aircraft measurements in China. *Atmos. Environ.*, **45**, 665–672, doi: 10.1016/j.atmosenv.2010.10.025.

Zhang, R. J., Y. F. Xu, and Z. W. Han, 2003: Inorganic chemical composition and source signature of PM2.5 in Beijing during ACE-Asia period. *Chinese Science Bulletin*, **48**(10), 1002–1005.

Zhang, R. J., Z. W. Han, Z. X. Shen, and J. J. Cao, 2008: Continuous measurement of number concentrations and elemental composition of aerosol particles for a dust storm event in Beijing. *Adv. Atmos. Sci.*, **25**, 89–95, doi: 10.1007/s00376-008-0089-2.

Zhang, W. J., Y. L. Sun, G. S. Zhuang, and D. Q. Xu, 2006: Characteristics and seasonal variations of PM2.5, PM10, and TSP aerosol in Beijing. *Biomed. Environ. Sci.*, **19**, 461–468.

Zhang, H, Z. Shen, X. Wei, M. Zhang, and Z. Li, 2012a: Comparison of optical properties of nitrate and sulfate aerosol and the direct radiative forcing due to nitrate in China. *Atmospheric Research*, **113**, 113–125.

Zhang, H., and Coauthors, 2012b: Simulation of direct radiative forcing of aerosols and their effects on East Asian climate using an interactive AGCM-aerosol coupled system. *Climate Dyn.*, **38**, 1675–1693.

Zhang, X. Y., J. J. Cao, and L. M. Li, 2002: Characterization of atmospheric aerosol over XiAn in the south margin of the Loess Plateau, China. *Atmos. Environ.*, **36**(26), 4189–4199.

Zhang, X. Y., Y. Q. Wang, T. Niu, X. C. Zhang, S. L. Gong, Y. M. Zhang, and J. Y. Sun, 2012c: Atmospheric aerosol compositions in China: Spatial/temporal variability, chemical signature, regional haze distribution and comparisons with global aerosols. *Atmos. Chem. Phys.*, **12**, 779–799.

Zhao, C. S., X. X. Tie, and Y. P. Lin, 2006: A possible positive feedback of reduction of precipitation and increase in aerosols over eastern central China. *Geophys. Res. Lett.*, **33**, L11814, doi: 10.1029/2006GL025959.

Zheng, X., W. M. Kang, T. L. Zhao, Y. X. Luo, C. C. Duan, and J. Chen, 2008: Long-term trends in sunshine duration over Yunnan-Guizhou Plateau in Southwest China for 1961–2005. *Geophys. Res. Lett.*, **35**, L15707, doi: 10.1029/2008GL 034482.

Zhu, J. L., H. Liao, and J. P. Li, 2012: Increases in aerosol concentrations over eastern China due to the decadal-scale weakening of the East Asian summer monsoon. *Geophys. Res. Lett.*, **39**, L09809, doi: 10.1029/2012GL051428.

Zhuang, B. L., F. Jiang, T. J. Wang, S. Li, and B. Zhu, 2011: Investigation on the direct radiative effect of fossil fuel black-carbon aerosol over China. *Theor. Appl. Climatol.*, **104**, 301–312, doi: 10.1007/s00704-010-0341-4.

Zhuang, B. L., Q. Liu, T. J. Wang, Q. Yin, S. Li, M. Xie, and F. Jiang, 2013: Investigation on semi-direct and indirect climate effects of fossil fuel black carbon aerosol over China. *Theor. Appl. Climatol.*, **114**, 651–672, doi: 10.1007/s00704-013-0862-8.